Title: Incentives modulate arousal and attention in risky choice

Authors: Abdelaziz Alsharawy[1], Xiaomeng Zhang[2], Sheryl Ball[3,4], Alec Smith[3,4]*

Affiliations:

[1]School of Public and International Affairs, Princeton University; Princeton, NJ, USA

[2]Economics Experimental Lab, Nanjing Audit University; Nanjing, China

[3]Department of Economics, Virginia Tech; Blacksburg, VA, USA

[4]School of Neuroscience, Virginia Tech; Blacksburg, VA, USA

***** Corresponding author. Email: alecsmith@vt.edu

October 15th, 2021

Abstract: We investigated the effect of large changes in financial incentives on the process of decision-making by measuring autonomic arousal and visual attention during an incentivized lottery-choice task. High real stakes were accompanied by increased risk aversion and physiological arousal, and by shifts in attention toward safer alternatives. These effects were manifested both within and between individuals. We find no evidence that heightened risk aversion is a mistake. To capture the interactions of arousal and attention with subjective value during evidence accumulation, we developed and fit a new arousal-modulated Attentional Drift Diffusion model (aADDM). Our computational model demonstrates that arousal amplifies discounting of high-valued outcomes when participants attended to low-valued outcomes. Arousal and attention, and their interaction, are integral to the process of decision-making under risk.

One sentence summary: High stakes decrease risk taking, increase autonomic arousal, and shift attention, with arousal amplifying attentional biases.

Main Text:

Important decisions, such as whether to run from a bear or to sell stocks during a market crash, involve high stakes and risk. In the most widely used models of decision making, choices are determined by stable preferences (*1*) and result from the cognitive evaluation of risk and reward. However, the decision environment itself may influence the choice process via changes in affect (*2*, *3*). Emotional responses involve fluctuations in autonomic arousal, which in turn is associated with widespread changes in both physiology and cognition (*4*, *5*). Arousal is linked to changes in both incentives (*6*, *7*) and uncertainty (*8–10*) and is likely an adaptive response to changes in the distribution of rewards in the environment (*8*, *11*).

According to the Yerkes-Dodson relationship, task performance is optimized at intermediate levels of arousal (*12*, *4*). In financial decision-making, high stakes typically lead to increased behavioral risk aversion (*13*, *14*). Incentives increase mental effort and can improve performance in cognitive tasks (*15*). However, high stakes also lead to mistakes (*16*, *17*). Hence, high-stakes risk aversion may be a rational response to increased incentives (*18*, *19*) in resource-constrained decision-making (*20*), or it might be a decision bias (*21*) resulting from hyper-arousal (*17*, *22*).

Arousal is also linked to increased attention to salient or goal-relevant stimuli (*23*, *24*). Both elevated arousal and attention to losses are associated with increased loss aversion (*25–28*), but it is not clear how arousal might influence attention allocation and the process of decision-making between risky choices that do not involve losses. To pin down the changes in the decision process that characterize high stakes risk aversion, we measured arousal, attention, and attitudes towards risk while experiment participants chose between two lotteries, one safe and one risky, each with two strictly positive payoffs, from the well-known task of Holt & Laury (2002) (see Table S1). Prior to participating in each block of 20 choice trials, participants learned the specific payoffs (Figs. 1A-B) and whether a randomly determined choice would be selected for real payment. The high hypothetical (Block 2) and high real (Block 3) conditions involved the same 10 lottery choices (repeated twice in two randomly ordered sub-blocks) as in the low real blocks (1 and 4), but with payoffs multiplied by 50. During the task, we recorded reaction time, choice consistency, gaze fixation, pupil dilation, pulse rate, and skin conductance from N=46 participants (median age=21, 28 males, 7 excluded due to data collection problems – see supplementary material) (Fig. 1C). We hypothesized that large changes in stakes would generate a pronounced autonomic response, and that this response would be associated with both increased risk aversion and changes in the decision-making process.

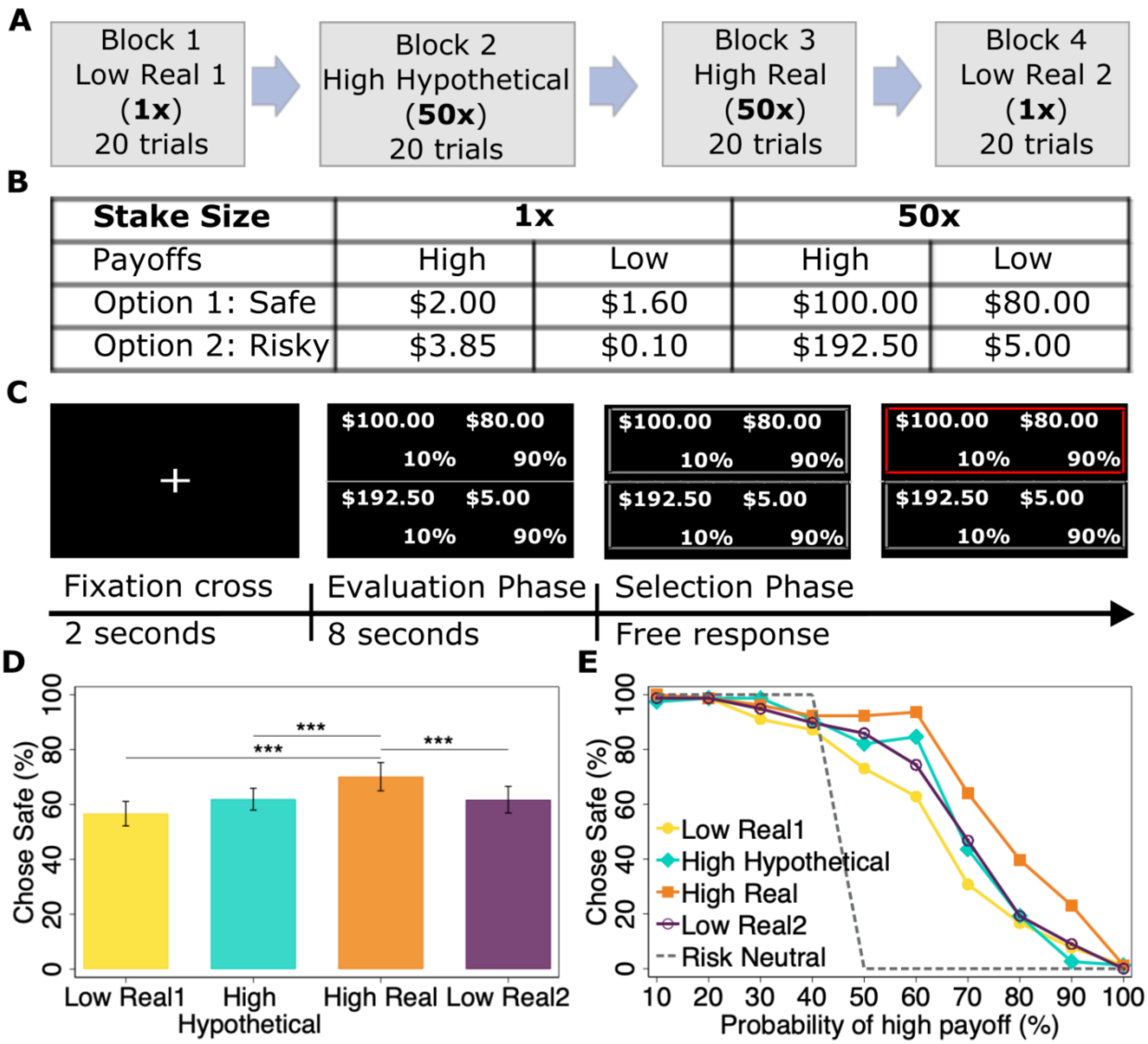

Fig. 1. Task and behavior (A) *Participants completed four blocks of paired lottery-choice decisions in order. The probability of the high payoff varied between 10% to 100%. Each choice (see Table S1) was presented twice, in sub-blocks of 10. The presentation format (left vs. right; top vs. bottom) and the order of the lottery-choice decisions within each sub-block were randomized across participants.* ***(B)*** *High payoffs (both hypothetical and real) were generated by multiplying the low payoffs by a scale factor of 50.* ***(C)*** *Example of a single decision round.* ***(D)*** *The rate of choosing the safe lottery across blocks and* ***(E)***

*for each lottery-choice decision ordered by the probability of the high payoff (participant means). Implied risk aversion was greatest in the high real condition (Wilcoxon signed-rank test, N=39: *** P-value < 0.001). Error bars denote 95% confidence intervals.*

Participants chose the safe option more frequently in the high stakes block ($M_{difference}$>8%; Wilcoxon signed-rank test: N=39, all P<0.001; Fig. 1D-E), consistent with previously reported behavioral findings (*13*, *14*) and in contrast to models that imply scale invariance (*29*). To examine the causal effect of incentives on arousal, we measured pulse rate, skin conductance, and pupil dilation, prior to stimulus presentation while participants viewed a fixation cross (see Fig. 1C). All three measures of pretrial arousal were significantly higher when stakes were high and real ($M_{difference}$>0.332; Wilcoxon signed-rank test: N=39, all P<0.010) (Fig. 2A and Fig. S2). Since the three arousal measures were highly correlated, we computed their first principal component (pc1) to capture generalized arousal (see the supplementary material for procedures, and for data on phasic arousal). Individual differences in the effect of high stakes on implied risk aversion (mean number of safe choices in high real minus hypothetical) were positively and significantly associated with changes in arousal (Fig. 2B; Spearman rank correlation: N=39; ρ_s=0.441, P=0.005).

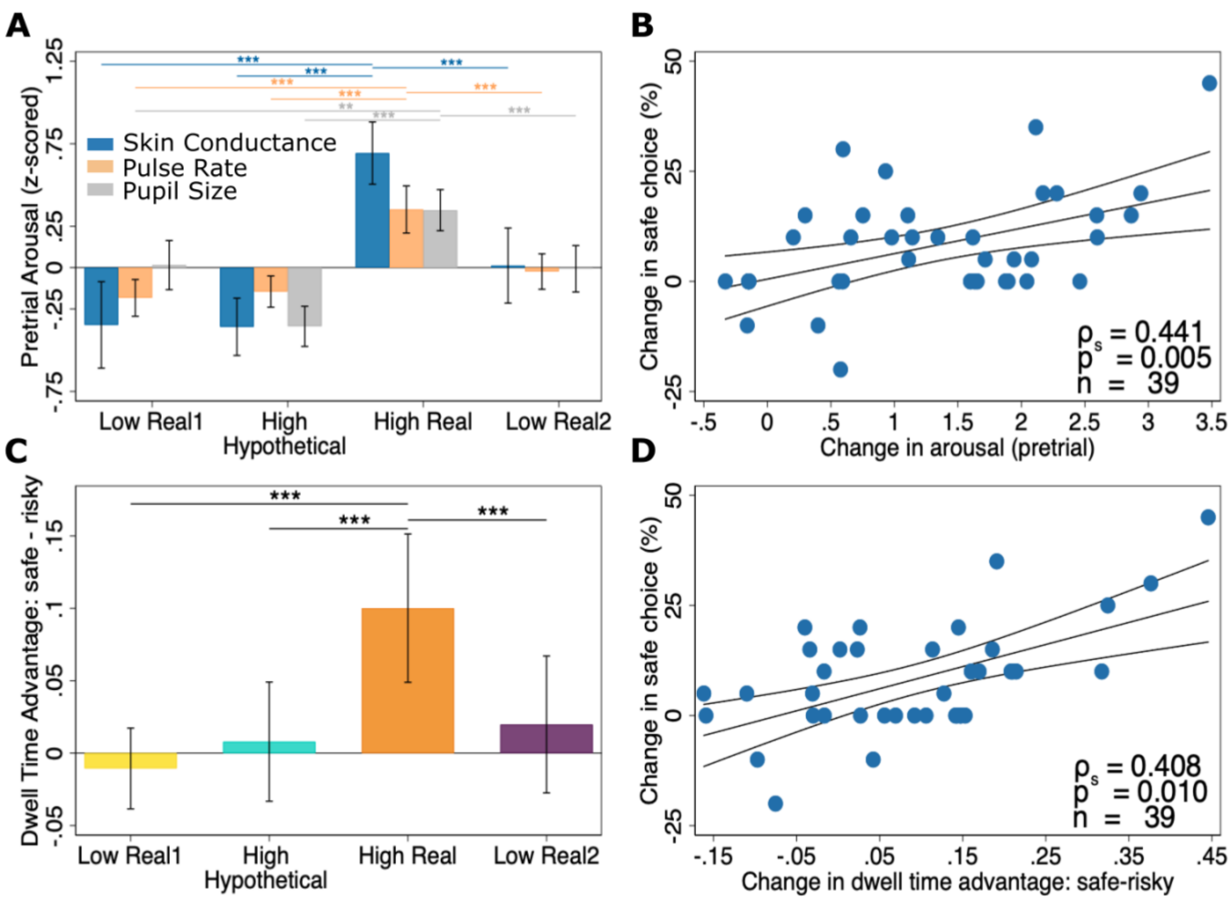

Fig. 2. Incentives, arousal, and attention. (A) *Skin conductance, pulse rate, and pupil diameter were all higher under high real stakes.* ***(B)*** *Individual differences in the effect of high stakes on generalized arousal were strongly associated with changes in risk aversion. The percentage difference in safe choices (y-axis) in the high real vs. the hypothetical block is plotted against the change in arousal (x-axis). Generalized arousal is computed as the first principal component of the three pretrial arousal measures (pc1): skin conductance, pulse rate, and pupil size.* ***(C)*** *Dwell time advantage during the evaluation phase for the safe option (relative fixation duration on safe outcomes minus risky outcomes) was highest during the high real block.* ***(D)*** *Individual differences in the effect of high stakes on dwell time advantage for the safe option in the high real vs. the*

hypothetical block (x-axis) were strongly associated with changes in risk aversion (y-axis). Spearman rank correlation and linear fits plotted in ***(B)*** *and* ***(D)****. Error bars and line bounds show 95% confidence intervals. For* ***(A)*** *and* ***(C)****, Wilcoxon signed-rank test (N=39): ** P-value < 0.01; *** P-value < 0.001.*

Gaze bias, whereby people tend to select the option that they have attended to the most, is a robust phenomenon in both simple and risky choice (*25*, *30–33*). In our experiment, participants fixated significantly more on the safe option in the high real block ($M_{difference}$>0.080; Wilcoxon signed-rank test: N=39, all P<0.001) (Fig. 2C and Fig. S4). Individual differences in implied risk aversion in the real vs. the hypothetical block were also positively and significantly associated with increases in dwell time for the safe option (Spearman rank correlation: N=39; ρ_s =0.408, P=0.010) (Fig. 2D).

High stakes also caused fixations to vary between attributes of the lotteries. Participants fixated relatively less on the risky high outcome and more on both outcomes of the safe option, in high real vs. hypothetical (risky high: $M_{difference} = 0.039$, safe high: $M_{difference}$ =0.018, safe low: $M_{difference}$ =0.028; Wilcoxon signed-rank test: N=39, all P<0.051) (Fig. 3A). When participants chose the safe option, there was a gradual trend toward fixating more on both safe payoffs. However, when participants chose the risky option, there was an immediate and persistent fixation bias toward the risky high payoff (Figs. 3B-C, S5 and, S6). This difference might reflect resource rational attention allocation (*20*), as the contribution of the risky low payoff to the computation of expected utility is low, regardless of the probability of this outcome occurring.

Importantly, we find no evidence that increased risk aversion under high stakes is a mistake. On the contrary, the percentage of participants making inconsistent choices (i.e. selecting different options for the same decision within a block) was marginally lower under high real stakes (Blocks 3 and 2: $M_{difference}$=4.103; Wilcoxon signed-rank test: N=39, P=0.066; Blocks 3 and 1: $M_{difference}$=12.051, P<0.001; Blocks 3 and 4: $M_{difference}$=2.564, P>0.100) (see Fig. 3D). We also compute the Payne index of visual information processing on each trial (*34*). Larger values of the index indicate more alternative-based evaluation and less reliance on heuristics. The average Payne index was greater under high real stakes compared to the high hypothetical (Block 2) and second low real block (Block 4) ($M_{difference}$=0.030, 0.049, respectively; Wilcoxon signed-rank test: N=39, both P<0.003) (see Fig. 3E). High stakes also resulted in increased reaction time, after controlling for the overall downward trend during the experiment (see Fig. S7). Taken together, these results suggest that high stakes increased both arousal and mental effort (*15*).

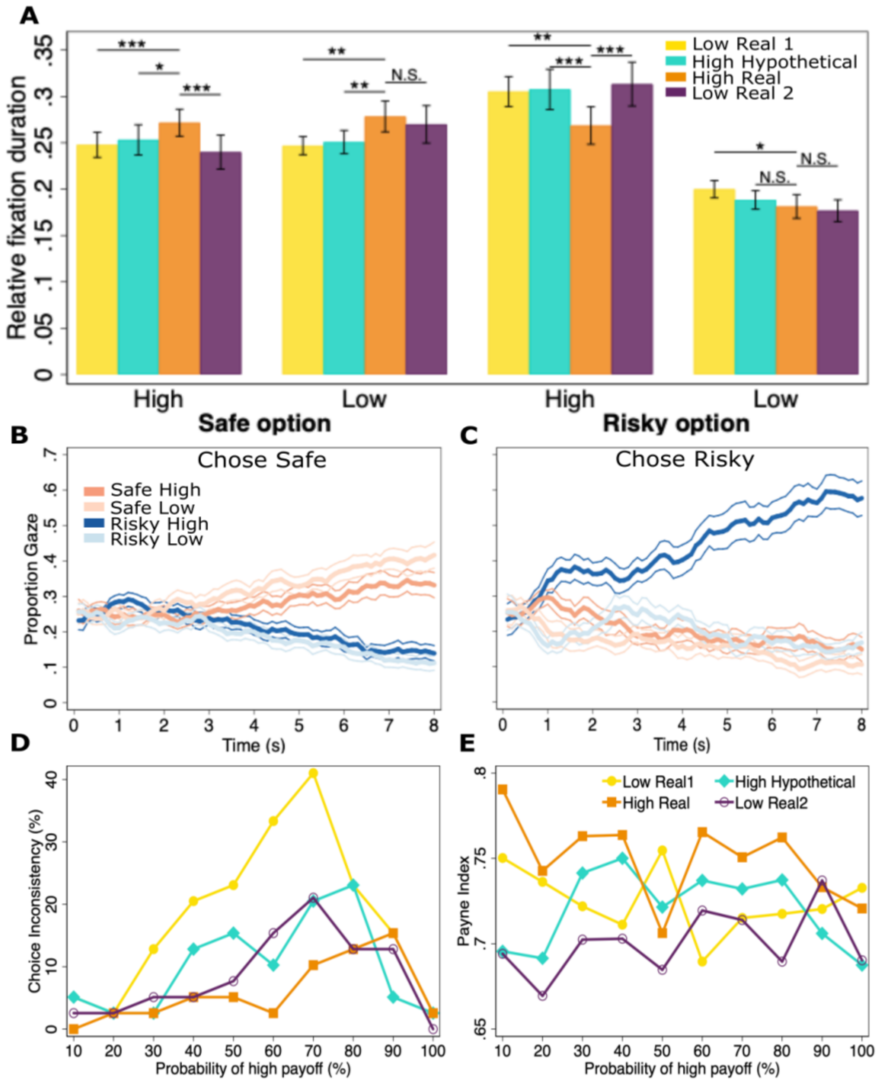

Fig. 3. Incentives and the choice process. (A) *Relative fixation duration (dwell-time proportion) on each outcome and associated probability during the evaluation phase. Fixation duration on the risky high outcome decreased in the high real block relative to the other three blocks. Fixation duration on the risky low outcome remained relatively unchanged, and fixation duration on the safe high and low outcomes increased.* ***(B-C)*** *Cumulative proportion of the evaluation phase with gaze fixated on each outcome and associated probability when participants* ***(B)*** *chose the safe option and* ***(C)*** *chose the risky option. When choosing the safe option, participants fixated more on both the high and*

low outcomes of the safe option. When choosing the risky option, however, participants fixated more on only the risky high outcome. Data shown are pooled within 100-millisecond windows. ***(D)*** *Percentage of participants making inconsistent choices and* ***(E)*** *mean Payne index of each decision for each block. Overall, choice inconsistency declines and Payne index increases under high real stakes. Error bars and line bounds show 95% confidence intervals. Wilcoxon signed-rank test (N=39): * P-value < 0.05; ** P-value < 0.01; *** P-value < 0.001; N.S. not significant.*

Drift Diffusion Models (DDMs) link reaction times and choices by positing that the accumulation of evidence about the value of the options is a stochastic process (*35*). The decision threshold represents the amount of information required before making a choice, while the drift rate represents the speed by which a decision maker accumulates information. We ran a simple DDM that allows the threshold to vary with pre-trial arousal (pc1). Arousal increased the amount of information required to arrive at a decision, signifying higher response caution (*30*) ($\beta = 0.051, \mathrm{P} < 0.0001;$ $\mathrm{where\ P} = 1 - \mathrm{pd},$ $\mathrm{and\ pd\ is\ the\ posterior\ probability\ of\ direction}$) (Fig. 4A).

Extensions of the DDM incorporate the effect of visual attention on choice to demonstrate how gaze modulates value computations (*31*, *30*, *32*, *36*). Since autonomic arousal is thought to amplify the gain in information processing (*4*, *9*, *24*), we hypothesized that arousal would modulate gaze bias. To capture the interaction of arousal (pc1) and evaluation phase attention during evidence accumulation, we developed the arousal-modulated Attentional Drift Diffusion model (aADDM). We fit the model using hierarchical drift diffusion modeling (HDDM, see supplementary material) (*37*). The best fitting model, which closely matches observed data (see Fig. 4B-D and Fig. S8), allows for differential attention to high or low outcomes and interacts this attention with arousal.

High-valued outcomes were discounted steeply when attending to low outcomes, and arousal amplifies this bias (γ_{High} = *-4.96, P=0.005;* $\gamma_{pc1*High}$ = *-4.09, P=0.002* – $where\ P = 1 - pd$ – see supplementary material). On the other hand, low-valued outcomes were not discounted when participants attended to high outcomes, and there was no interaction with arousal (see Fig. 4E and Table S2; see Fig. S9 for models derived using selection phase gaze). These findings demonstrate that physiological arousal modulates the interaction of value and visual attention in risky choice such that the most informative attributes contribute more to evidence accumulation.

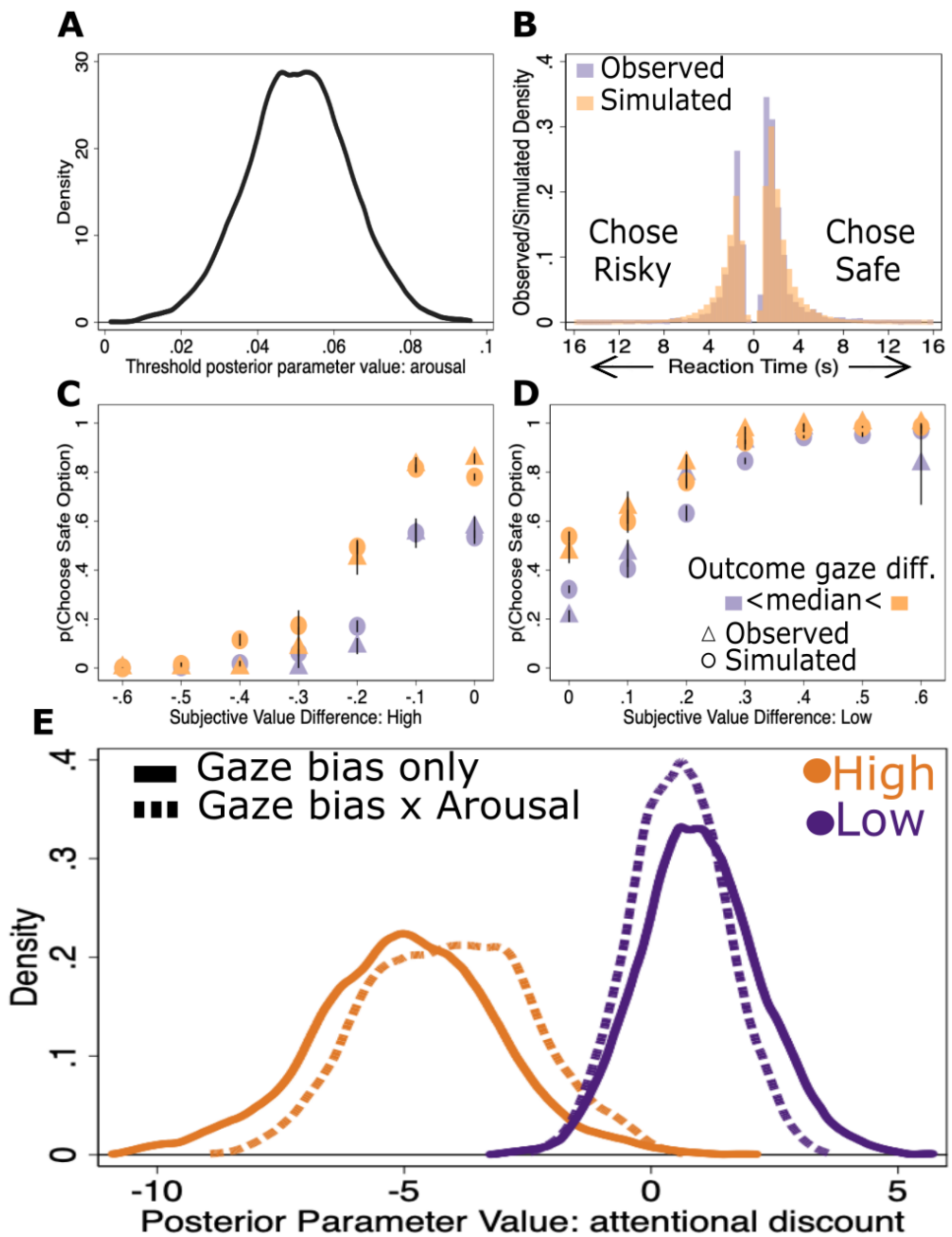

Fig. 4. Arousal-modulated Attentional Drift Diffusion Model (A) *Arousal increased the decision threshold ($\beta = 0.051, P < 0.0001$) in a simple drift-diffusion model.* ***(B-D)*** *Simulated choices from the best fitting model (see supplementary material) predicted* ***(B)*** *reaction time and* ***(C)*** *observed choices relative to the high outcomes' value difference, and* ***(D)*** *the low outcomes' value difference. Error spikes denote the standard error of the mean. Extreme outlier reaction times are not shown in (B), less than 1.3% of the data*

points are omitted. ***(E)*** *Gaze on the opposite outcome during the evaluation phase discounted the value of the high outcomes only (γ_{High}= -4.96, P (1-pd)=0.005). Generalized arousal amplified the high outcomes' attentional bias during the evaluation phase ($\gamma_{pc1tonic*High}$= -4.09, P (1-pd)=0.002) (see the supplementary material for details).*

References

1. G. J. Stigler, G. S. Becker, De gustibus non est disputandum. *The american economic review*. **67**, 76–90 (1977).

2. G. F. Loewenstein, E. U. Weber, C. K. Hsee, N. Welch, Risk as feelings. *Psychological Bulletin*. **127**, 267–286 (2001).

3. E. A. Phelps, K. M. Lempert, P. Sokol-Hessner, Emotion and decision making: multiple modulatory neural circuits. *Annual review of neuroscience*. **37**, 263–287 (2014).

4. G. Aston-Jones, J. D. Cohen, An integrative theory of locus coeruleus-norepinephrine function: adaptive gain and optimal performance. *Annu. Rev. Neurosci.* **28**, 403–450 (2005).

5. A. B. Satpute, P. A. Kragel, L. F. Barrett, T. D. Wager, M. Bianciardi, Deconstructing arousal into wakeful, autonomic and affective varieties. *Neuroscience Letters*. **693**, 19–28 (2019).

6. D. Kahneman, W. S. Peavler, Incentive effects and pupillary changes in association learning. *Journal of Experimental Psychology*. **79**, 312 (1969).

7. M. Richter, G. H. Gendolla, The heart contracts to reward: Monetary incentives and preejection period. *Psychophysiology*. **46**, 451–457 (2009).

8. A. J. Yu, P. Dayan, Uncertainty, Neuromodulation, and Attention. *Neuron*. **46**, 681–692 (2005).

9. M. R. Nassar, K. M. Rumsey, R. C. Wilson, K. Parikh, B. Heasly, J. I. Gold, Rational regulation of learning dynamics by pupil-linked arousal systems. *Nature neuroscience*. **15**, 1040 (2012).

10. A. E. Urai, A. Braun, T. H. Donner, Pupil-linked arousal is driven by decision uncertainty and alters serial choice bias. *Nature communications*. **8**, 1–11 (2017).

11. T. Parr, K. J. Friston, Uncertainty, epistemics and active inference. *Journal of the Royal Society Interface*. **14**, 20170376 (2017).

12. R. M. Yerkes, J. D. Dodson, The relation of strength of stimulus to rapidity of habit-formation. *Journal of comparative neurology and psychology*. **18**, 459–482 (1908).

13. H. P. Binswanger, Attitudes toward risk: Experimental measurement in rural India. *American journal of agricultural economics*. **62**, 395–407 (1980).

14. C. A. Holt, S. K. Laury, Risk Aversion and Incentive Effects. *The American Economic Review*. **92**, 1644–1655 (2002).

15. A. Shenhav, S. Musslick, F. Lieder, W. Kool, T. L. Griffiths, J. D. Cohen, M. M. Botvinick, Toward a rational and mechanistic account of mental effort. *Annual review of neuroscience*. **40**, 99–124 (2017).

16. R. F. Baumeister, Choking under pressure: Self-consciousness and paradoxical effects of incentives on skillful performance. *Journal of Personality and Social Psychology*. **46**, 610–620 (1984).

17. D. Ariely, U. Gneezy, G. Loewenstein, N. Mazar, Large Stakes and Big Mistakes. *The Review of Economic Studies*. **76**, 451–469 (2009).

18. M. Rabin, Risk Aversion and Expected-utility Theory: A Calibration Theorem. *Econometrica*. **68**, 1281–1292 (2000).

19. M. Bombardini, F. Trebbi, Risk aversion and expected utility theory: an experiment with large and small stakes. *Journal of the European Economic Association*. **10**, 1348–1399 (2012).

20. R. Bhui, L. Lai, S. J. Gershman, Resource-rational decision making. *Current Opinion in Behavioral Sciences*. **41**, 15–21 (2021).

21. E. Eldar, V. Felso, J. D. Cohen, Y. Niv, A pupillary index of susceptibility to decision biases. *Nature Human Behaviour*, 1–10 (2021).

22. S. Dunne, V. S. Chib, J. Berleant, J. P. O'Doherty, Reappraisal of incentives ameliorates choking under pressure and is correlated with changes in the neural representations of incentives. *Social cognitive and affective neuroscience*. **14**, 13–22 (2019).

23. E. Eldar, J. D. Cohen, Y. Niv, The effects of neural gain on attention and learning. *Nature neuroscience*. **16**, 1146–1153 (2013).

24. M. Mather, D. Clewett, M. Sakaki, C. W. Harley, Norepinephrine ignites local hotspots of neuronal excitation: How arousal amplifies selectivity in perception and memory. *Behavioral and Brain Sciences*. **39** (2016).

25. S. Fiedler, A. Glöckner, The dynamics of decision making in risky choice: An eye-tracking analysis. *Frontiers in psychology*. **3**, 335–335 (2012).

26. F. Sheng, A. Ramakrishnan, D. Seok, W. J. Zhao, S. Thelaus, P. Cen, M. L. Platt, Decomposing loss aversion from gaze allocation and pupil dilation. *Proceedings of the National Academy of Sciences*. **117**, 11356–11363 (2020).

27. P. Sokol-Hessner, M. Hsu, N. G. Curley, M. R. Delgado, C. F. Camerer, E. A. Phelps, Thinking like a trader selectively reduces individuals' loss aversion. *Proceedings of the National Academy of Sciences*. **106**, 5035–5040 (2009).

28. G. Hochman, E. Yechiam, Loss aversion in the eye and in the heart: The autonomic nervous system's responses to losses. *Journal of behavioral decision making*. **24**, 140–156 (2011).

29. M. W. Khaw, Z. Li, M. Woodford, Cognitive imprecision and small-stakes risk aversion. *The review of economic studies*. **88**, 1979–2013 (2021).

30. J. F. Cavanagh, T. V. Wiecki, A. Kochar, M. J. Frank, Eye tracking and pupillometry are indicators of dissociable latent decision processes. *Journal of Experimental Psychology: General*. **143**, 1476–1476 (2014).

31. I. Krajbich, C. Armel, A. Rangel, Visual fixations and the computation and comparison of value in simple choice. *Nature neuroscience*. **13**, 1292–1292 (2010).

32. S. M. Smith, I. Krajbich, Gaze Amplifies Value in Decision Making. *Psychological Science*. **30**, 116–128 (2019).

33. N. Stewart, F. Hermens, W. J. Matthews, Eye movements in risky choice. *Journal of behavioral decision making*. **29**, 116–136 (2016).

34. J. W. Payne, M. L. Braunstein, Risky choice: An examination of information acquisition behavior. *Memory & Cognition*. **6**, 554–561 (1978).

35. R. Ratcliff, P. L. Smith, S. D. Brown, G. McKoon, Diffusion decision model: Current issues and history. *Trends in cognitive sciences*. **20**, 260–281 (2016).

36. A. Westbrook, R. van den Bosch, J. Määttä, L. Hofmans, D. Papadopetraki, R. Cools, M. J. Frank, Dopamine promotes cognitive effort by biasing the benefits versus costs of cognitive work. *Science*. **367**, 1362–1366 (2020).

37. T. V. Wiecki, I. Sofer, M. J. Frank, HDDM: hierarchical bayesian estimation of the drift-diffusion model in python. *Frontiers in neuroinformatics*. **7**, 14–14 (2013).

38. P. R. Murphy, I. H. Robertson, J. H. Balsters, R. G. O'connell, Pupillometry and P3 index the locus coeruleus–noradrenergic arousal function in humans. *Psychophysiology*. **48**, 1532–1543 (2011).

39. R. Hou, C. Freeman, R. Langley, E. Szabadi, C. Bradshaw, Does modafinil activate the locus coeruleus in man? Comparison of modafinil and clonidine on arousal and autonomic functions in human volunteers. *Psychopharmacology*. **181**, 537–549 (2005).

40. J. Beatty, Task-evoked pupillary responses, processing load, and the structure of processing resources. *Psychological bulletin*. **91**, 276–276 (1982).

41. M. M. Bradley, L. Miccoli, M. A. Escrig, P. J. Lang, The pupil as a measure of emotional arousal and autonomic activation. *Psychophysiology*. **45**, 602–607 (2008).

42. E. Eldar, J. D. Cohen, Y. Niv, The effects of neural gain on attention and learning. *Nature neuroscience*. **16**, 1146–1153 (2013).

43. D. C. Fowles, M. J. Christie, R. Edelberg, W. W. Grings, D. T. Lykken, P. H. Venables, Publication recommendations for electrodermal measurements. *Psychophysiology*. **18**, 232–239 (1981).

44. J. Allen, Photoplethysmography and its application in clinical physiological measurement. *Physiological measurement*. **28**, R1 (2007).

45. J. J. Braithwaite, D. G. Watson, R. Jones, M. Rowe, A guide for analysing electrodermal activity (EDA) & skin conductance responses (SCRs) for psychological experiments. *Psychophysiology*. **49**, 1017–1034 (2013).

46. J. R. Jennings, W. K. Berg, J. S. Hutcheson, P. Obrist, S. Porges, G. Turpin, Publication guidelines for heart rate studies in man. *Psychophysiology*. **18**, 226–231 (1981).

47. M. J. Frank, C. Gagne, E. Nyhus, S. Masters, T. V. Wiecki, J. F. Cavanagh, D. Badre, fMRI and EEG predictors of dynamic decision parameters during human reinforcement learning. *Journal of Neuroscience*. **35**, 485–494 (2015).

48. I. Krajbich, C. Armel, A. Rangel, Visual fixations and the computation and comparison of value in simple choice. *Nature neuroscience*. **13**, 1292 (2010).

49. J. F. Cavanagh, T. V Wiecki, A. Kochar, M. J. Frank, Eye tracking and pupillometry are indicators of dissociable latent decision processes. *Journal of Experimental Psychology: General*. **143**, 1476 (2014).

50. F. Sheng, A. Ramakrishnan, D. Seok, W. J. Zhao, S. Thelaus, P. Cen, M. L. Platt, Decomposing loss aversion from gaze allocation and pupil dilation. *Proceedings of the National Academy of Sciences*. **117**, 11356–11363 (2020).

51. S. M. Smith, I. Krajbich, Attention and choice across domains. *Journal of Experimental Psychology: General*. **147**, 1810–1810 (2018).

52. A. Saha, Expo-power utility: A 'flexible'form for absolute and relative risk aversion. *American Journal of Agricultural Economics*. **75**, 905–913 (1993).

53. D. Luce, Individual choice behavior (1959).

54. K. C. Armel, A. Beaumel, A. Rangel, Biasing simple choices by manipulating relative visual attention. *Judgment and Decision making*. **3**, 396–403 (2008).

55. A. Arieli, Y. Ben-Ami, A. Rubinstein, Tracking decision makers under uncertainty. *American Economic Journal: Microeconomics*. **3**, 68–76 (2011).

56. J. A. Aimone, S. Ball, B. King-Casas, It's not what you see but how you see it: Using eye-tracking to study the risky decision-making process. *Journal of Neuroscience, Psychology, and Economics*. **9**, 137–137 (2016).

57. F. M. Howells, D. J. Stein, V. A. Russell, Synergistic tonic and phasic activity of the locus coeruleus norepinephrine (LC-NE) arousal system is required for optimal attentional performance. *Metabolic brain disease*. **27**, 267–274 (2012).

Funding: Funding provided by the Virginia Tech Department of Economics.

Conflicts of Interest/Competing Interests: The authors declare that they have no conflicts of interest/competing interests.

Author contributions: Conceptualization: A.A., X.Z., S.B., A.S., Methodology: A.A., S.B., A.S., Software: A.A., X.Z., S.B., A.S., Investigation: A.A., X.Z., Formal Analysis: A.A., A.S., Visualization: A.A., A.S., Validation: A.A., A.S., Data Curation: A.A., Resources: S.B., A.S., Funding acquisition: A.S., Project administration: A.S., Supervision: S.B., A.S., Writing – Original Draft: A.A., A.S., Writing – Review & Editing: A.A., S.B., A.S.

Availability of data and materials: Data and materials will be made available via the Open Science Framework upon publication.

Code Availability: Code will be made available via the Open Science Framework upon publication.

Supplementary Materials

Materials and Methods

Supplementary Test

Fig. S1 – S9

Table S1 – S2

References (38 – 57)

Supplementary Materials for

Incentives modulate arousal and attention in risky choice

Abdelaziz Alsharawy, Xiaomeng Zhang, Sheryl Ball, Alec Smith

Correspondence to: alecsmith@vt.edu

This PDF file includes:

Supplementary Materials

Materials and Methods

Subjects

All procedures were approved by Virginia Tech Institutional Review Board, and each participant provided informed consent prior to participation. There was no deception involved in this study. The average payment received by participants was $108.58, which includes $10 show-up fee. Each participant made a total of 80 lottery choices, using Holt & Laury (2002) (*14*) lotteries (see Table S1). Initially we recruited 46 participants but data from 39 were used in our final analysis, as seven participants from our original sample were excluded due to either poor eye tracking data (5 participants), stimulus computer crash (1 participant) or non-responsive skin conductance measurement (1 participant). Thus, our analysis sample included 24 males and 15 females with an average age of 22 (minimum age: 18, maximum age: 33).

Task

We only used two stake sizes from Holt & Laury's (2002) original lottery choices: the low stake size (1X) and a high-stake size of 50X (the exact payoffs in each stake size condition are shown in Fig. 1B of the main text). Our experiment employs a within-subject design in which each participant completes four blocks in the following order (see Fig. 1A of the main text):

1) Low Real1 (1X): 20 low stakes choices with one choice randomly selected for payment.
2) High Hypothetical (50X): 20 hypothetical choices of the high payoffs.
3) High Real (50X): 20 high stakes choices with one choice randomly selected for payment.
4) Low Real2 (1X): 20 low stakes choices with one choice randomly selected for payment.

Participants were presented with the lottery choices sequentially. The order of the lotteries within a block is randomized across participants who see each decision problem twice, once in the first 10 trials and once again in the second 10 trials. To help ensure that participants scan all the information on the screen and that the presentation format is not causing a bias, we add variation in the presentation format as follows: for each of the first 10 trials, a random number determines which of the presentation formats is used with an equal chance of each of the following: 1) the safe lottery up and the high payoffs to the left, 2) the safe lottery up and the high payoffs to the right, 3) the safe lottery down and the high payoffs to the left, and 4) the safe lottery down and the high payoffs to the right. In the second 10 trials in a block, we show the same 10 payoffs and associated probabilities again but with the opposite presentation format. A participant, for example, who sees one of the decision problems with the safe lottery up and the large payoffs to the left during the first 10 trials, would be presented with the same decision problem but with the safe lottery down and the large payoffs to the right during the second 10 trials. The order of the lottery choices within a block is randomized across participants for the first 10 trials and again for the next 10 trials. The order of the four blocks, however, is the same for all participants.

Prior to moving to the next block, one lottery from the completed block is randomly selected and realized to determine the payoff for that block. In order to proceed to the high real block and to control for wealth effects, participants had to agree to forfeit the first block's payment before they proceeded. Unsurprisingly, all participants elected to forfeit their first block's payment. For the high hypothetical block, we asked participants to acknowledge that the payoffs in that block were hypothetical and will not be paid. Also, to familiarize participants with the payoff structure associated with that upcoming block, one random trial from the block was presented during the instruction phase of that block and prior to making decisions.

Procedures

After participants arrive in the lab and complete the consent phase, we first connect the transducers that measure heart rate and skin conductance to three fingers on the left hand. The next step is the calibration and validation process for the EyeLink 1000 plus eye tracker, which typically takes 5 to 10 minutes. This step is important in accurately collecting gaze data. Next, participants are presented with the instructions that are specific to the block they will see. During each trial, a fixation cross appears at the center of the screen for 2 seconds before the two options are presented on the screen for 8 seconds (Evaluation Phase: EP) (see Fig. 1C in the main text). Pretrial psychophysiological measured during the presentation of the fixation cross reflect tonic level of arousal, and arousal measured during the Evaluation Phase reflect phasic arousal level (*38*). Pupillometry studies, for example, show that drugs that induce low arousal decrease baseline pupil diameter (Hou et al., 2005) whereas responding to stimuli in cognitive tasks rapidly increases pupil size (Beatty, 1982). After 8 seconds, two rectangular grey boxes appear on the screen, one for each option. Participants had unlimited time to use the arrow keys on the keyboard, causing the box on the selected option to become red, until selecting the option that they prefer by pressing the Enter button (Selection Phase: SP). Once an option is submitted, a fixation cross appears again before the next trial is presented. Reaction time was recorded once the rectangular grey boxes appear on the screen. Each participant was informed of each block's outcome before reading the instructions for the next block. The mean duration of the experimental session was around 50 minutes.

Eye-tracking and Physiological Measurements

Presentation of the gambles and the selection of options were programmed using Matlab, employing Psychophysics and Eyelink toolbox extensions (http://psychtoolbox.org/) to record eye movements and pupil dilation. We collected eye tracking data using the EyeLink 1000 Plus eye tracker, which consists of a High-Speed Camera that records 1000 samples per second and a Host PC that is dedicated to receiving and processing the collected data (see http://www.sr-research.com/mount_desktop_1000plus.html for more information). We used a desktop mount that sits in front of the stimulus monitor, and we employ an adjustable head stabilizer (chin rest) to improve data quality. Participants face the camera, which is placed in front of the monitor. Prior to the presentation of each decision, a fixation cross appears on the monitor for 2 seconds as highlighted in the previous section. Pretrial pupil dilation is measured as the baseline mean pupil size 1 second before stimulus presentation while evaluation phase (phasic) pupil dilation is measured as the difference between maximum pupil size recorded in the evaluation phase and the pretrial (tonic) pupil size (Fig. S1) (*38*, *41*, *42*). We then compute pretrial pupil size and evaluation phase pupil dilation z-scores for each participant.

Physiological data on pulse rate and skin conductance were collected using the software Aqcknowledge version 5.0.4, BIOPAC MP160WSW data acquisition system and BioNomadix PPG & EDA system. The data was recorded at 2000 samples per second (see www.biopac.com for details). The following physiological measures were collected via wireless devices worn on the left hand: Electrodermal Activity (EDA) and Pulse Photoplethysmogram (PPG) (*43*, *44*). EDA (also known as Galvanic Skin Response (GSR) or Skin Conductance Activity (SCA)) is a measure of eccrine activity or skin sweating. EDA signal can be obtained from placing two electrodes (Ag-

AgCl) on two different fingers of the hand while very low constant voltage is applied (which is not felt by the participant). The constant voltage is maintained between the two electrodes such that current flow is proportional to skin conductance (*45*). We placed the (disposable) electrodes on the ring and middle fingers of the left hand (between the middle and distal phalanges). Before exporting the data for analysis in Stata 15.1, we used the software Aqcknowledge version 5.0.4 to filter and smooth the data and to mark skin conductance responses.

EDA data were down sampled to 250 Hz before further analysis. We derived pretrial Skin Conductance Level (SCL) as a one second mean of skin conductance before stimulus presentation and during fixation cross presentation (*41*, *45*). Moreover, we set a minimal response criterion at 0.02 μS (microSiemens), and we measured evaluation phase skin conductance response (SCR) as the maximum recorded response by trough-to-peak amplitude difference in the time window 1 second after the presentation of the lotteries in a trial till 8 seconds from onset (Fig. S1). SCL relates to the general level of skin conductance, which reacts slowly, while SCR reacts faster to presented stimuli (*45*). For data processing, we applied the following: low-pass filtering (25 Hz), smoothing (3 sample kernel), and applying a square root transformation (*27*). We then estimate a z-score for each participant to facilitate comparisons within and across participants. Thus, we derive our two measures (z-score) of skin conductance: 1) pretrial skin conductance level and 2) evaluation phase skin conductance responses.

PPG provides measurements for pulse rate and is measured via a wireless transducer that monitors changes in infrared reflectance resulting from varying blood flow. The pulse transducer was placed on the index finger's distal phalange of the same hand where the electrodes were placed. The PPG signal was down sampled (250 Hz) and smoothed (3 sample kernel) before deriving the pulse rate using a minimum threshold of 0.05 volts. The pulse rate signal was also smoothed (3 sample kernel). Similar to skin conductance, we computed the mean pretrial measure of heart rate as a one second average before stimulus presentation (*46, 41*). We then compute the mean pulse rate recorded during the first 8 seconds from stimuli presentation onset (Fig. S1). And, we generate an analogous phasic (change from baseline) pulse rate measure by subtracting the pretrial measure of pulse rate from the 8 second mean evaluation phase pulse rate. For consistency, we refer to this measure as evaluation phase pulse rate. Last, we derived pretrial and evaluation phase pulse rate z-scores for each participant.

HDDM estimation

HDDM involves Markov Chain Monte-Carlo (MCMC) sampling to estimate DDM parameters for both individual and group-level. To avoid an explosion in the number of parameters and to aid in convergence, we only estimate individual estimates for the intercept in the drift rate regression and we obtain group estimates for the remaining regression coefficients (*47*). In the HDDM estimation for all our models, we used 6000 samples drawn from the posterior and discarded the first 1000 samples as burn-in. In our models, we fit participant's choice (safe/risky) along with reaction time and we fit regression models for drift rate as outlined in the subsequent section. To investigate how trial-to-trial changes in arousal levels influence the decision threshold, we also run a separate model that fits a regression model for threshold with pretrial arousal as a regressor (DIC=11864).

aADDM

Our arousal-modulated Attentional Drift Diffusion Model (aADDM) integrates arousal to previously developed sequential sampling models (*48–50*, *36*). Estimated subjective utilities have been used to substitute objective values when the latter cannot always be identified and has been implemented in an application to risky choice experiments (*51*). Thus, we resort to estimating subjective utilities for each outcome, and each option, using power-expo utility function ($U(x) = \frac{1-\exp(-\alpha x^{1-r})}{\alpha}$) given the functional form's superiority in modelling increased risk aversion with increased stakes (*52*, *14*). Note that both constant relative risk aversion and constant absolute risk aversion are special cases in the power-expo model when α and r converge to zero, respectively. Power-expo utility function allows for the common finding of increasing relative risk aversion and decreasing absolute risk aversion.

Using observations from real blocks only, we fit a nonlinear mixed effects model using maximum likelihood (menl function in Stata 15.1) to estimate each participant's α and r parameters in the power-expo function while including an individual level noise parameter μ (*53*). We specify an unstructured covariance structure between the random intercepts α, r and μ, and we estimate an exchangeable covariance structure for within-subject errors. For μ approaching zero, the option with the higher expected utility is chosen with certainty while for larger values of μ, the probability of choosing that option converges to one-half. The trial likelihood function involved estimating the probability of choosing the top option presented on the screen such that: $pr(choosing\ top\ option) = \frac{U_{top}^{\frac{1}{\mu}}}{U_{top}^{\frac{1}{\mu}} + U_{bottom}^{\frac{1}{\mu}}}$ and $U_{\{top,bottom\}}$ are formulated using the power-expo utility function weighted by the probabilities of each outcome. Note that decisions from the hypothetical block were omitted during the estimation procedure. The individual estimates of α and r were then used to compute subjective utilities for each outcome that were later used in the HDDM estimation: subjective values (sv) for the safe high (SH), risky high (RH), safe low (SL) and risky low (RL) (sv_{SH}, sv_{RH}, sv_{SL}, sv_{RL}, respectively). We normalize the subjective values for each individual between 0 (lowest value) and 1 (highest value). Outcomes' subjective values were then summed up to derive the subjective value for each of the options (sv_{safe}, sv_{risky}) that were used in the option-wise models. Two participants (out of 39) had estimates of r that were greater than 1. For both participants, we divided their subjective values by 1-r before adding twice the lowest subjective value estimated for each participant. This helped us ensure that for all participants, a more positive value indicates higher subjective value with a subjective value of zero given only when the probability of receiving the payoff is zero. These steps were necessary for applying our normalization technique that is consistent across our participants. Our results remain the same if we, instead, exclude these two participants from our analysis.

We estimate both option-wise and attribute-wise models to analyze the decision process of choosing the safe option while allowing for attentional bias to influence evidence accumulation. Equations SE1-SE3 outline the option-wise models' specification for the drift rate (v_{ij}, participant i in trial j), while equations SE4-SE6 outline that of the attribute-wise models. Equations SE1PC1-SE6PC1 outline the drift rate specifications that allow pretrial arousal (first principal component of the arousal measures – $pc1$) to modulate all other included variables.

In model SE1 (option-wise additive), we allow the drift rate to vary with the value difference between the safe (sv_{safe}) and risky (sv_{risky}) options. Also, we include additive (simple) gaze bias: relative fixation duration spent on the safe option (g_{safe}) minus that spent on the risky one (g_{risky}). In model SE2 (option-wise multiplicative), we allow the values of the fixated option (fix) to be integrated differently from the values of non-fixated option ($nonfix$). In model SE3 (option-wise additive and multiplicative), we allow both additive and multiplicative gaze to influence the decision process.

Model SE1: $$\mathbf{v_{ij}} = \boldsymbol{\beta}_{\mathbf{0i}} + \boldsymbol{\beta}_{\mathbf{sv}}\left(\mathbf{sv_{safe}} - \mathbf{sv_{risky}}\right)_{\mathbf{j}} + \boldsymbol{\beta}_{\boldsymbol{\Delta}\mathbf{g}}\left(\mathbf{g_{safe}} - \mathbf{g_{risky}}\right)_{\mathbf{j}}$$

Model SE1PC1: $$\mathbf{v_{ij}} = \boldsymbol{\beta}_{\mathbf{0i}} + \boldsymbol{\beta}_{\mathbf{pc1}}\mathbf{pc1}_{\boldsymbol{j}} + \boldsymbol{\beta}_{\mathbf{sv}}\left(\mathbf{sv_{safe}} - \mathbf{sv_{risky}}\right)_{\mathbf{j}} + \boldsymbol{\beta}_{\mathbf{sv*pc1}}\left(\mathbf{sv_{safe}} - \mathbf{sv_{risky}}\right)_{\mathbf{j}} * \mathbf{pc1}_{\boldsymbol{j}} + \boldsymbol{\beta}_{\boldsymbol{\Delta}\mathbf{g}}\left(\mathbf{g_{safe}} - \mathbf{g_{risky}}\right)_{\mathbf{j}} + \boldsymbol{\beta}_{\boldsymbol{\Delta}\mathbf{g*pc1}}\left(\mathbf{g_{safe}} - \mathbf{g_{risky}}\right)_{\mathbf{j}} * \mathbf{pc1}_{\boldsymbol{j}}$$

Model SE2: $$\mathbf{v_{ij}} = \boldsymbol{\beta}_{\mathbf{0j}} + \boldsymbol{\beta}_{\mathbf{fix}}\left(\mathbf{g_{safe}} * \mathbf{sv_{safe}} - \mathbf{g_{risky}} * \mathbf{sv_{risky}}\right)_{\mathbf{j}} + \boldsymbol{\beta}_{\mathbf{nonfix}}\left(\mathbf{g_{risky}} * \mathbf{sv_{safe}} - \mathbf{g_{safe}} * \mathbf{sv_{risky}}\right)_{\mathbf{j}}$$

Model SE2PC1: $$\mathbf{v_{ij}} = \boldsymbol{\beta}_{\mathbf{0j}} + \boldsymbol{\beta}_{\mathbf{pc1}}\mathbf{pc1}_{\boldsymbol{j}} + \boldsymbol{\beta}_{\mathbf{fix}}\left(\mathbf{g_{safe}} * \mathbf{sv_{safe}} - \mathbf{g_{risky}} * \mathbf{sv_{risky}}\right)_{\mathbf{j}} + \boldsymbol{\beta}_{\mathbf{fix*pc1}}\left(\mathbf{g_{safe}} * \mathbf{sv_{safe}} - \mathbf{g_{risky}} * \mathbf{sv_{risky}}\right)_{\mathbf{j}} * \mathbf{pc1}_{\boldsymbol{j}} + \boldsymbol{\beta}_{\mathbf{nonfix}}\left(\mathbf{g_{risky}} * \mathbf{sv_{safe}} - \mathbf{g_{safe}} * \mathbf{sv_{risky}}\right)_{\mathbf{j}} + \boldsymbol{\beta}_{\mathbf{nonfix*pc1}}\left(\mathbf{g_{risky}} * \mathbf{sv_{safe}} - \mathbf{g_{safe}} * \mathbf{sv_{risky}}\right)_{\mathbf{j}} * \mathbf{pc1}_{\boldsymbol{j}}$$

Model SE3 $$\boldsymbol{v_{ij}} = \boldsymbol{\beta}_{\mathbf{0j}} + \boldsymbol{\beta}_{\mathbf{fix}}\left(\mathbf{g_{safe}} * \mathbf{sv_{safe}} - \mathbf{g_{risky}} * \mathbf{sv_{risky}}\right)_{\mathbf{j}} + \boldsymbol{\beta}_{\mathbf{nonfix}}\left(\mathbf{g_{risky}} * \mathbf{sv_{safe}} - \mathbf{g_{safe}} * \mathbf{sv_{risky}}\right)_{\mathbf{j}} + \boldsymbol{\beta}_{\boldsymbol{\Delta}\mathbf{g}}\left(\mathbf{g_{safe}} - \mathbf{g_{risky}}\right)_{\mathbf{j}}$$

Model SE3PC1 $$\mathbf{v_{ij}} = \boldsymbol{\beta}_{\mathbf{0j}} + \boldsymbol{\beta}_{\mathbf{pc1}}\mathbf{pc1}_{\boldsymbol{j}} + \boldsymbol{\beta}_{\mathbf{fix}}\left(\mathbf{g_{safe}} * \mathbf{sv_{safe}} - \mathbf{g_{risky}} * \mathbf{sv_{risky}}\right)_{\mathbf{j}} + \boldsymbol{\beta}_{\mathbf{fix*pc1}}\left(\mathbf{g_{safe}} * \mathbf{sv_{safe}} - \mathbf{g_{risky}} * \mathbf{sv_{risky}}\right)_{\mathbf{j}} * \mathbf{pc1}_{\boldsymbol{j}} + \boldsymbol{\beta}_{\mathbf{nonfix}}\left(\mathbf{g_{risky}} * \mathbf{sv_{safe}} - \mathbf{g_{safe}} * \mathbf{sv_{risky}}\right)_{\mathbf{j}} + \boldsymbol{\beta}_{\mathbf{nonfix*pc1}}\left(\mathbf{g_{risky}} * \mathbf{sv_{safe}} - \mathbf{g_{safe}} * \mathbf{sv_{risky}}\right)_{\mathbf{j}} * \mathbf{pc1}_{\boldsymbol{j}} + \boldsymbol{\beta}_{\boldsymbol{\Delta}\mathbf{g}}\left(\mathbf{g_{safe}} - \mathbf{g_{risky}}\right)_{\mathbf{j}} + \boldsymbol{\beta}_{\boldsymbol{\Delta}\mathbf{g*pc1}}\left(\mathbf{g_{safe}} - \mathbf{g_{risky}}\right)_{\mathbf{j}} * \mathbf{pc1}_{\boldsymbol{j}}$$

We also run attribute-wise variant models where attention to the high outcomes (high payoffs and their associated probabilities) in the presented lotteries are allowed to influence the decision process differently compared to attention to the low outcomes. These models are useful in examining whether visual attention directed at particular attributes in decision problems influence evidence accumulation differently (*36*). Equations SE4-SE5 and SE6 outline the specification models for the drift rate (v_{ij}) in our attribute-wise models for the decision process of choosing the safe option. In model SE4 (attribute-wise additive), we allow the drift rate to differ across high and low outcomes. In particular, the evaluation of the high outcomes of the safe ($sv_{safe_{High}}$) and that of the risky option ($sv_{Risky_{High}}$) influence the drift rate differently compared to the evaluation of the low outcome of the safe option ($sv_{safe_{Low}}$) and that of the risky option ($sv_{Risky_{Low}}$). In addition, we include a term for the gaze difference of attending to the safe option's high outcome ($g_{safe_{High}}$) instead of the risky option's high outcome ($g_{Risky_{High}}$) and another analogous term for attending to the safe option's low outcome ($g_{safe_{Low}}$) instead of the risky option's low outcome ($g_{Risky_{Low}}$). This represents simple (additive) gaze bias that is independent of the particular attribute value but is again allowed to influence drift rate differently for high and low outcomes. In model SE5 (attribute-wise multiplicative), we allow the subjective value differences, between 1) safe high (g_{SH}) and risky high (g_{RH}) and 2) safe low (g_{SL}) and risky low (g_{RL}), to be evaluated at different rates when fixating on the same attribute (sameA), or the other attribute (otherA), of the same option (sameO) or of the other option (otherO). Importantly, we estimate different weights for the evaluation of the high outcomes (H) compared to that of the low outcomes (L). In model SE6 (attribute-wise additive and multiplicative), we allow both additive and multiplicative gaze to influence evidence accumulation. Each variable in this last model (SE6) is then interacted with arousal (SE6PC1) and yields the results reported in main text. This is the model that provides the best model fits for both evaluation phase and selection phase gaze (see Fig. S8).

Model SE4: $\mathbf{v_{ij}} = \boldsymbol{\beta}_{\mathbf{0j}} + \boldsymbol{\beta}_{\mathbf{High}}\left(\mathbf{sv}_{\mathbf{safe_{High}}} - \mathbf{sv}_{\mathbf{Risky_{High}}}\right)_{\mathbf{j}} + \boldsymbol{\beta}_{\mathbf{Low}}\left(\mathbf{sv}_{\mathbf{safe_{Low}}} - \mathbf{sv}_{\mathbf{Risky_{Low}}}\right)_{\mathbf{j}} + \boldsymbol{\beta}_{\boldsymbol{\Delta}\mathbf{g_{High}}}\left(\mathbf{g}_{\mathbf{safe_{High}}} - \mathbf{g}_{\mathbf{Risky_{High}}}\right)_{\mathbf{j}} + \boldsymbol{\beta}_{\boldsymbol{\Delta}\mathbf{g_{Low}}}\left(\mathbf{g}_{\mathbf{safe_{Low}}} - \mathbf{g}_{\mathbf{Risky_{Low}}}\right)_{\mathbf{j}}$

Model SE4PC1: $\mathbf{v_{ij}} = \boldsymbol{\beta}_{\mathbf{0j}} + \boldsymbol{\beta}_{\mathbf{pc1}}\mathbf{pc1_j} + \boldsymbol{\beta}_{\mathbf{High}}\left(\mathbf{sv}_{\mathbf{safe_{High}}} - \mathbf{sv}_{\mathbf{Risky_{High}}}\right)_{\mathbf{j}} + \boldsymbol{\beta}_{\mathbf{High*pc1}}\left(\mathbf{sv}_{\mathbf{safe_{High}}} - \mathbf{sv}_{\mathbf{Risky_{High}}}\right)_{\mathbf{j}} * \mathbf{pc1_j} + \boldsymbol{\beta}_{\mathbf{Low}} * \left(\mathbf{sv}_{\mathbf{safe_{Low}}} - \mathbf{sv}_{\mathbf{Risky_{Low}}}\right)_{\mathbf{j}} + \boldsymbol{\beta}_{\mathbf{Low*pc1}}\left(\mathbf{sv}_{\mathbf{safe_{Low}}} - \mathbf{sv}_{\mathbf{Risky_{Low}}}\right)_{\mathbf{j}} * \mathbf{pc1_j} + \boldsymbol{\beta}_{\boldsymbol{\Delta}\mathbf{g_{High}}}\left(\mathbf{g}_{\mathbf{safe_{High}}} - \mathbf{g}_{\mathbf{Risky_{High}}}\right)_{\mathbf{j}} + \boldsymbol{\beta}_{\boldsymbol{\Delta}\mathbf{g_{High}*pc1}}\left(\mathbf{g}_{\mathbf{safe_{High}}} - \mathbf{g}_{\mathbf{Risky_{High}}}\right)_{\mathbf{j}} * \mathbf{pc1_j} + \boldsymbol{\beta}_{\boldsymbol{\Delta}\mathbf{g_{Low}}}\left(\mathbf{g}_{\mathbf{safe_{Low}}} - \mathbf{g}_{\mathbf{Risky_{Low}}}\right)_{\mathbf{j}} + \boldsymbol{\beta}_{\boldsymbol{\Delta}\mathbf{g_{Low}*pc1}}\left(\mathbf{g}_{\mathbf{safe_{Low}}} - \mathbf{g}_{\mathbf{Risky_{Low}}}\right)_{\mathbf{j}} * \mathbf{pc1_j}$

Model SE5: $\mathbf{v_{ij}} = \boldsymbol{\beta}_{\mathbf{0j}} + \boldsymbol{\beta}_{\mathbf{H_{sameO_{sameA}}}}\left(\mathbf{g_{SH}sv}_{\mathbf{safe_{High}}} - \mathbf{g_{RH}sv}_{\mathbf{Risky_{High}}}\right)_{\mathbf{j}} + \boldsymbol{\beta}_{\mathbf{H_{sameO_{otherA}}}}\left(\mathbf{g_{SL}sv}_{\mathbf{safe_{High}}} - \mathbf{g_{RL}sv}_{\mathbf{Risky_{High}}}\right)_{\mathbf{j}} + \boldsymbol{\beta}_{\mathbf{H_{otherO_{sameA}}}}\left(\mathbf{g_{RH}sv}_{\mathbf{safe_{High}}} - \mathbf{g_{SH}sv}_{\mathbf{Risky_{High}}}\right)_{\mathbf{j}} + \boldsymbol{\beta}_{\mathbf{H_{otherO_{otherA}}}}\left(\mathbf{g_{RL}sv}_{\mathbf{safe_{High}}} - \mathbf{g_{SL}sv}_{\mathbf{Risky_{High}}}\right)_{\mathbf{j}} + \boldsymbol{\beta}_{\mathbf{L_{sameO_{sameA}}}}\left(\mathbf{g_{SL}sv}_{\mathbf{safe_{Low}}} - \mathbf{g_{RL}sv}_{\mathbf{Risky_{Low}}}\right)_{\mathbf{j}} + \boldsymbol{\beta}_{\mathbf{L_{sameO_{otherA}}}}\left(\mathbf{g_{SH}sv}_{\mathbf{safe_{Low}}} - \mathbf{g_{RH}sv}_{\mathbf{Risky_{Low}}}\right)_{\mathbf{j}} + \boldsymbol{\beta}_{\mathbf{L_{otherO_{sameA}}}}\left(\mathbf{g_{RL}sv}_{\mathbf{safe_{Low}}} - \mathbf{g_{SL}sv}_{\mathbf{Risky_{Low}}}\right)_{\mathbf{j}} + \boldsymbol{\beta}_{\mathbf{L_{otherO_{otherA}}}}\left(\mathbf{g_{RH}sv}_{\mathbf{safe_{Low}}} - \mathbf{g_{SH}sv}_{\mathbf{Risky_{Low}}}\right)_{\mathbf{j}}$

Model SE5PC1: $\mathbf{v_{ij}} = \boldsymbol{\beta}_{\mathbf{0j}} + \boldsymbol{\beta}_{\mathbf{pc1}}\mathbf{pc1_j} + \boldsymbol{\beta}_{\mathbf{H_{sameO_{sameA}}}}\left(\mathbf{g_{SH}sv}_{\mathbf{safe_{High}}} - \mathbf{g_{RH}sv}_{\mathbf{Risky_{High}}}\right)_{\mathbf{j}} + \boldsymbol{\beta}_{\mathbf{H_{sameO_{sameA}}*pc1}}\left(\mathbf{g_{SH}sv}_{\mathbf{safe_{High}}} - \mathbf{g_{RH}sv}_{\mathbf{Risky_{High}}}\right)_{\mathbf{j}} * \mathbf{pc1_j} + \boldsymbol{\beta}_{\mathbf{H_{sameO_{otherA}}}}\left(\mathbf{g_{SL}sv}_{\mathbf{safe_{High}}} - \mathbf{g_{RL}sv}_{\mathbf{Risky_{High}}}\right)_{\mathbf{j}} + \boldsymbol{\beta}_{\mathbf{H_{sameO_{otherA}}*pc1}}\left(\mathbf{g_{SL}sv}_{\mathbf{safe_{High}}} - \mathbf{g_{RL}sv}_{\mathbf{Risky_{High}}}\right)_{\mathbf{j}} * \mathbf{pc1_j} + \boldsymbol{\beta}_{\mathbf{H_{otherO_{sameA}}}}\left(\mathbf{g_{RH}sv}_{\mathbf{safe_{High}}} - \mathbf{g_{SH}sv}_{\mathbf{Risky_{High}}}\right)_{\mathbf{j}} + \boldsymbol{\beta}_{\mathbf{H_{otherO_{sameA}}*pc1}}\left(\mathbf{g_{RH}sv}_{\mathbf{safe_{High}}} - \mathbf{g_{SH}sv}_{\mathbf{Risky_{High}}}\right)_{\mathbf{j}} * \mathbf{pc1_j} + \boldsymbol{\beta}_{\mathbf{H_{otherO_{otherA}}}}\left(\mathbf{g_{RL}sv}_{\mathbf{safe_{High}}} - \mathbf{g_{SL}sv}_{\mathbf{Risky_{High}}}\right)_{\mathbf{j}} + \boldsymbol{\beta}_{\mathbf{H_{otherO_{otherA}}*pc1}}\left(\mathbf{g_{RL}sv}_{\mathbf{safe_{High}}} - \mathbf{g_{SL}sv}_{\mathbf{Risky_{High}}}\right)_{\mathbf{j}} * \mathbf{pc1_j} + \boldsymbol{\beta}_{\mathbf{L_{sameO_{sameA}}}}\left(\mathbf{g_{SL}sv}_{\mathbf{safe_{Low}}} - \mathbf{g_{RL}sv}_{\mathbf{Risky_{Low}}}\right)_{\mathbf{j}} + \boldsymbol{\beta}_{\mathbf{L_{sameO_{sameA}}*pc1}}\left(\mathbf{g_{SL}sv}_{\mathbf{safe_{Low}}} - \mathbf{g_{RL}sv}_{\mathbf{Risky_{Low}}}\right)_{\mathbf{j}} * \mathbf{pc1_j} + \boldsymbol{\beta}_{\mathbf{L_{sameO_{otherA}}}}\left(\mathbf{g_{SH}sv}_{\mathbf{safe_{Low}}} - \mathbf{g_{RH}sv}_{\mathbf{Risky_{Low}}}\right)_{\mathbf{j}} + \boldsymbol{\beta}_{\mathbf{L_{sameO_{otherA}}*pc1}}\left(\mathbf{g_{SH}sv}_{\mathbf{safe_{Low}}} - \mathbf{g_{RH}sv}_{\mathbf{Risky_{Low}}}\right)_{\mathbf{j}} * \mathbf{pc1_j} + \boldsymbol{\beta}_{\mathbf{L_{otherO_{sameA}}}}\left(\mathbf{g_{RL}sv}_{\mathbf{safe_{Low}}} - \mathbf{g_{SL}sv}_{\mathbf{Risky_{Low}}}\right)_{\mathbf{j}} + \boldsymbol{\beta}_{\mathbf{L_{otherO_{sameA}}*pc1}}\left(\mathbf{g_{RL}sv}_{\mathbf{safe_{Low}}} - \mathbf{g_{SL}sv}_{\mathbf{Risky_{Low}}}\right)_{\mathbf{j}} * \mathbf{pc1_j} + \boldsymbol{\beta}_{\mathbf{L_{otherO_{otherA}}}}\left(\mathbf{g_{RH}sv}_{\mathbf{safe_{Low}}} - \mathbf{g_{SH}sv}_{\mathbf{Risky_{Low}}}\right)_{\mathbf{j}} + \boldsymbol{\beta}_{\mathbf{L_{otherO_{otherA}}*pc1}}\left(\mathbf{g_{RH}sv}_{\mathbf{safe_{Low}}} - \mathbf{g_{SH}sv}_{\mathbf{Risky_{Low}}}\right)_{\mathbf{j}} * \mathbf{pc1_j}$

Model SE6: $\mathbf{v_{ij}} = \boldsymbol{\beta}_{\mathbf{0j}} + \boldsymbol{\beta}_{\mathbf{H_{sameO_{sameA}}}}\left(\mathbf{g_{SH}sv}_{\mathbf{safe_{High}}} - \mathbf{g_{RH}sv}_{\mathbf{Risky_{High}}}\right)_{\mathbf{j}} + \boldsymbol{\beta}_{\mathbf{H_{sameO_{otherA}}}}\left(\mathbf{g_{SL}sv}_{\mathbf{safe_{High}}} - \mathbf{g_{RL}sv}_{\mathbf{Risky_{High}}}\right)_{\mathbf{j}} + \boldsymbol{\beta}_{\mathbf{H_{otherO_{sameA}}}}\left(\mathbf{g_{RH}sv}_{\mathbf{safe_{High}}} - \mathbf{g_{SH}sv}_{\mathbf{Risky_{High}}}\right)_{\mathbf{j}} + \boldsymbol{\beta}_{\mathbf{H_{otherO_{otherA}}}}\left(\mathbf{g_{RL}sv}_{\mathbf{safe_{High}}} - \mathbf{g_{SL}sv}_{\mathbf{Risky_{High}}}\right)_{\mathbf{j}} + \boldsymbol{\beta}_{\mathbf{L_{sameO_{sameA}}}}\left(\mathbf{g_{SL}sv}_{\mathbf{safe_{Low}}} - \mathbf{g_{RL}sv}_{\mathbf{Risky_{Low}}}\right)_{\mathbf{j}} + \boldsymbol{\beta}_{\mathbf{L_{sameO_{otherA}}}}\left(\mathbf{g_{SH}sv}_{\mathbf{safe_{Low}}} - \mathbf{g_{RH}sv}_{\mathbf{Risky_{Low}}}\right)_{\mathbf{j}} + \boldsymbol{\beta}_{\mathbf{L_{otherO_{sameA}}}}\left(\mathbf{g_{RL}sv}_{\mathbf{safe_{Low}}} - \mathbf{g_{SL}sv}_{\mathbf{Risky_{Low}}}\right)_{\mathbf{j}} + \boldsymbol{\beta}_{\mathbf{L_{otherO_{otherA}}}}\left(\mathbf{g_{RH}sv}_{\mathbf{safe_{Low}}} - \mathbf{g_{SH}sv}_{\mathbf{Risky_{Low}}}\right)_{\mathbf{j}} + \boldsymbol{\beta}_{\boldsymbol{\Delta}\mathbf{g_{High}}}\left(\mathbf{g}_{\mathbf{safe_{High}}} - \mathbf{g}_{\mathbf{Risky_{High}}}\right)_{\mathbf{j}} + \boldsymbol{\beta}_{\boldsymbol{\Delta}\mathbf{g_{Low}}}\left(\mathbf{g}_{\mathbf{safe_{Low}}} - \mathbf{g}_{\mathbf{Risky_{Low}}}\right)_{\mathbf{j}}$

Model SE6PC1: $\mathbf{v_{ij}} = \boldsymbol{\beta}_{\mathbf{0j}} + \boldsymbol{\beta}_{\mathbf{pc1}}\mathbf{pc1_j} + \boldsymbol{\beta}_{\mathbf{H_{sameO_{sameA}}}}\left(\mathbf{g_{SH}sv_{safe_{High}}} - \mathbf{g_{RH}sv_{Risky_{High}}}\right)_{\mathbf{j}} + \boldsymbol{\beta}_{\mathbf{H_{sameO_{sameA}}*pc1}}\left(\mathbf{g_{SH}sv_{safe_{High}}} - \mathbf{g_{RH}sv_{Risky_{High}}}\right)_{\mathbf{j}} * \mathbf{pc1_j} + \boldsymbol{\beta}_{\mathbf{H_{sameO_{otherA}}}}\left(\mathbf{g_{SL}sv_{safe_{High}}} - \mathbf{g_{RL}sv_{Risky_{High}}}\right)_{\mathbf{j}} + \boldsymbol{\beta}_{\mathbf{H_{sameO_{otherA}}*pc1}}\left(\mathbf{g_{SL}sv_{safe_{High}}} - \mathbf{g_{RL}sv_{Risky_{High}}}\right)_{\mathbf{j}} * \mathbf{pc1_j} + \boldsymbol{\beta}_{\mathbf{H_{otherO_{sameA}}}}\left(\mathbf{g_{RH}sv_{safe_{High}}} - \mathbf{g_{SH}sv_{Risky_{High}}}\right)_{\mathbf{j}} + \boldsymbol{\beta}_{\mathbf{H_{otherO_{sameA}}*pc1}}\left(\mathbf{g_{RH}sv_{safe_{High}}} - \mathbf{g_{SH}sv_{Risky_{High}}}\right)_{\mathbf{j}} * \mathbf{pc1_j} + \boldsymbol{\beta}_{\mathbf{H_{otherO_{otherA}}}}\left(\mathbf{g_{RL}sv_{safe_{High}}} - \mathbf{g_{SL}sv_{Risky_{High}}}\right)_{\mathbf{j}} + \boldsymbol{\beta}_{\mathbf{H_{otherO_{otherA}}*pc1}}\left(\mathbf{g_{RL}sv_{safe_{High}}} - \mathbf{g_{SL}sv_{Risky_{High}}}\right)_{\mathbf{j}} * \mathbf{pc1_j} + \boldsymbol{\beta}_{\mathbf{L_{sameO_{sameA}}}}\left(\mathbf{g_{SL}sv_{safe_{Low}}} - \mathbf{g_{RL}sv_{Risky_{Low}}}\right)_{\mathbf{j}} + \boldsymbol{\beta}_{\mathbf{L_{sameO_{sameA}}*pc1}}\left(\mathbf{g_{SL}sv_{safe_{Low}}} - \mathbf{g_{RL}sv_{Risky_{Low}}}\right)_{\mathbf{j}} * \mathbf{pc1_j} + \boldsymbol{\beta}_{\mathbf{L_{sameO_{otherA}}}}\left(\mathbf{g_{SH}sv_{safe_{Low}}} - \mathbf{g_{RH}sv_{Risky_{Low}}}\right)_{\mathbf{j}} + \boldsymbol{\beta}_{\mathbf{L_{sameO_{otherA}}*pc1}}\left(\mathbf{g_{SH}sv_{safe_{Low}}} - \mathbf{g_{RH}sv_{Risky_{Low}}}\right)_{\mathbf{j}} * \mathbf{pc1_j} + \boldsymbol{\beta}_{\mathbf{L_{otherO_{sameA}}}}\left(\mathbf{g_{RL}sv_{safe_{Low}}} - \mathbf{g_{SL}sv_{Risky_{Low}}}\right)_{\mathbf{j}} + \boldsymbol{\beta}_{\mathbf{L_{otherO_{sameA}}*pc1}}\left(\mathbf{g_{RL}sv_{safe_{Low}}} - \mathbf{g_{SL}sv_{Risky_{Low}}}\right)_{\mathbf{j}} * \mathbf{pc1_j} + \boldsymbol{\beta}_{\mathbf{L_{otherO_{otherA}}}}\left(\mathbf{g_{RH}sv_{safe_{Low}}} - \mathbf{g_{SH}sv_{Risky_{Low}}}\right)_{\mathbf{j}} + \boldsymbol{\beta}_{\mathbf{L_{otherO_{otherA}}*pc1}}\left(\mathbf{g_{RH}sv_{safe_{Low}}} - \mathbf{g_{SH}sv_{Risky_{Low}}}\right)_{\mathbf{j}} * \mathbf{pc1_j} + \boldsymbol{\beta}_{\mathbf{\Delta g_{High}}}\left(\mathbf{g_{safe_{High}}} - \mathbf{g_{Risky_{High}}}\right)_{\mathbf{j}} + \boldsymbol{\beta}_{\mathbf{\Delta g_{High}*pc1}}\left(\mathbf{g_{safe_{High}}} - \mathbf{g_{Risky_{High}}}\right)_{\mathbf{j}} * \mathbf{pc1_j} + \boldsymbol{\beta}_{\mathbf{\Delta g_{Low}}}\left(\mathbf{g_{safe_{Low}}} - \mathbf{g_{Risky_{Low}}}\right)_{\mathbf{j}} + \boldsymbol{\beta}_{\mathbf{\Delta g_{Low}*pc1}}\left(\mathbf{g_{safe_{Low}}} - \mathbf{g_{Risky_{Low}}}\right)_{\mathbf{j}} * \mathbf{pc1_j}$

In the main text, we report multiplicative attentional discounting of high and low outcomes. This bias was examined by computing the posterior parameter density for the following terms in equation SE6PC1: $\gamma_{\text{High}} = \beta_{\text{H}_{\text{sameO}_{\text{otherA}}}} + \beta_{\text{H}_{\text{otherO}_{\text{otherA}}}} - \beta_{\text{H}_{\text{sameO}_{\text{sameA}}}} - \beta_{\text{H}_{\text{otherO}_{\text{sameA}}}}$. Note that a negative γ_{High} provides evidence that high outcome values are being discounted when fixating on the low outcomes. Similarly, $\gamma_{\text{Low}} = \beta_{\text{L}_{\text{sameO}_{\text{otherA}}}} + \beta_{\text{L}_{\text{otherO}_{\text{otherA}}}} - \beta_{\text{L}_{\text{sameO}_{\text{sameA}}}} - \beta_{\text{L}_{\text{otherO}_{\text{sameA}}}}$ computes the attentional discounting low outcome evaluation while fixating on high outcomes. We then derive analgous posterior parameter densitites to investigate arousal's modulatory influence on attentional discounting across outcomes: $\gamma_{\text{pc1*High}} = \beta_{\text{pc1*H}_{\text{sameO}_{\text{otherA}}}} + \beta_{\text{pc1*H}_{\text{otherO}_{\text{otherA}}}} - \beta_{\text{pc1*H}_{\text{sameO}_{\text{sameA}}}} - \beta_{\text{pc1*H}_{\text{otherO}_{\text{sameA}}}}$ and $\gamma_{\text{pc1*Low}} = \beta_{\text{pc1*L}_{\text{sameO}_{\text{otherA}}}} + \beta_{\text{pc1*L}_{\text{otherO}_{\text{otherA}}}} - \beta_{\text{pc1*L}_{\text{sameO}_{\text{sameA}}}} - \beta_{\text{pc1*L}_{\text{otherO}_{\text{sameA}}}}$.

<u>Posterior Predictive Checks for aADDM</u>

Posterior predictive checks help in gauging the reliability of our model in producing observed behavioral patterns. We simulate 500 samples based on model estimates for each trial in our dataset. We generate two quantiles for evaluation phase 1) gaze bias on the safe option's high outcome instead of that of the risky option and 2) gaze bias on the safe option's low outcome instead of that of the risky option (Fig. 4 in the main manuscript). We analogously generate two quantiles using selection phase gaze to test the latter models (Fig. S9). Then, we compare the frequency of choosing the safe option across both observed and simulated datasets for both evaluation phase and selection phase models. The results provide visual evidence that our model simulations fare well in predicting behavior with regard to attribute-wise subjective value difference and for reaction time (Fig. 4 and Fig. S9).

Supplementary Text

<u>Physiological recordings and gaze bias within trials and across blocks</u>

We investigated how the trial's milli-second to milli-second arousal differed across blocks. Even though the general pattern of arousal was similar across blocks, the greatest arousal levels were recorded during the high real block (Figs. S1-S2). Note that under high real stakes, the phasic arousal measures, except for skin conductance response, did not significantly increase (see Fig. S3). By construct, the average pupil size and pulse rate phasic measures are inversely associated with their tonic (baseline) pretrial measures (*42*). The mild changes in phasic arousal under the high real stakes are in line with the Adaptive Gain Hypothesis, suggesting that high stakes may had instead induced a tonic high gain mode narrowing attention on the most strongly represented features of the lotteries (*4*, *42*). The increased evaluation phase gaze bias toward the safe option's attributes that we report in the main manuscript, and the selection phase gaze bias shown in Fig. S3, seems to suggest that the safe option is the pre-disposed sensory stimuli (see Fig. 3 in the main text).

Gaze bias (dwell time advantage for the safe option relative to the risky one) spiked at the beginning of the high real block before declining over subsequent trials (Figs. S4). Moreover, individual differences in changes in selection phase dwell time advantage from high hypothetical to high real block were strongly associated with increased risk aversion (Spearman rank correlation: n=39; ρ_s =0.873, P =4.3$\times 10^{-13}$). Similar to fixations during the evaluation phase (see Fig. 3 in main manuscript and Fig. S5), participants were attending more to the risky option's high payoff during selection phase when choosing the risky option (see Fig. S6).

Additive gaze bias

People are both influenced by what they look at but they also look at what they will choose (*36*, *54*). The former is accounted for by multiplicative gaze where attention boosts the value of fixated attributes, as reported in main text. The latter is accounted for by additive gaze where attention correlates to choice through a simple attention bias that is independent from value.

We find that simple gaze bias holds for both high and low outcomes (model SE6PC1), with the former having a larger impact on drift rate and with arousal interacting with evaluation phase gaze to widen this gap. For these additive gaze terms, an overall similar pattern prevails in both evaluation phase gaze and selection phase gaze, where more time spent fixating on high (low) outcomes of the safe option instead of the risky option's high (low) outcomes increases drift rate (EP: $\beta_{\Delta g_{high}} = 0.85, P < 0.0001$; $\beta_{\Delta g_{low}} = 0.79, P < 0.0001$; SP: $\beta_{\Delta g_{high}} = 1.39, P < 0.0001$; $\beta_{\Delta g_{low}} = 1.20, P < 0.0001$) with the former having a greater influence for SP gaze (EP:$\beta_{\Delta g_{high}} - \beta_{\Delta g_{low}} = 0.06, P = 0.333$; SP: $\beta_{\Delta g_{high}} - \beta_{\Delta g_{low}} = 0.19, P = 0.019$) (Fig. S9). Interestingly, we find that pretrial arousal does modulate additive EP gaze by enhancing its effect for high outcomes and weakening it for low outcomes ($\beta_{pc1*\Delta g_{high}} = 0.12, P = 0.053$; $\beta_{pc1*\Delta g_{low}} = -0.22, P = 0.010$). We thus find that arousal modulates both multiplicative and additive gaze bias during the evaluation phase of decision-making, amplifying attentional bias for high outcomes' value integration while also modulating additive gaze terms.

Direction of search

Standard models of risky choice assume that agents employ a particular cognitive processing patterns (expectation models) where people weigh the subjective value (utility) of the available option by its likelihood of occurrence to compute an expected utility associated with each option for choosing the one that maximizes welfare (*2*). In lottery choices, a strategy to choose the option with the higher expected utility is likely to involve more option-wise transitions (looking between attributes of the same alternative) rather than attribute-wise transitions (comparing probabilities or comparing payoffs across alternatives) that are typically associated with the usage of decision heuristics (*34*, *55*). Manipulating search strategy by presenting information that encourage within alternative-based transitions had been found to increase risk tolerance, establishing causal relationship between attention and risk decision making (*56*). As highlighted in the main text, we compute the Payne index, which has a larger score when transitions are more consistent with option-wise scan of information instead of attribute-wise ones (*34*).

Using a median split, we then created two groups based on the change in the average first principal component for the pretrial arousal measures from hypothetical to high real block. Then, we investigate how the change in information acquisition patterns altered behavior differently across participants who had low changes in arousal compared to those experiencing high changes. In the subsequent analysis, we focus our attention on the hypothetical and high real blocks and on decision numbers 5 to 9 in which behavior differs the most during the high real stakes block (see Fig. 1E in main text) and where the expectation value model predicts choosing the risky option (see Table S1). We find a negative and significant association between the change in Payne index from high hypothetical to the high real block and the change in risk aversion for the highly aroused participants (Spearman rank correlation: N=19; $\rho_s =$-0.737; P=0.0003) while no relationship was found for the modestly aroused group (Spearman rank correlation: N =20; $\rho_s =$0.136; P =0.568). Thus, the change in information acquisition patterns are strong predictors for adhering with the expectation model for participants experiencing heightened arousal only, where more option-wise scans were strongly associated with choosing the risky option. In addition, we examine whether changes in evaluation phase arousal (first principal component of evaluation phase arousal measures) impact information acquisition and risk aversion differently across the two groups. Interestingly, we find that only highly (pretrial) aroused participants had a positive and significant relationship between the change in evaluation phase arousal and increased risk aversion (Spearman rank correlation: N =19; $\rho_s =$0.566; P=0.012) and a negative and significant relationship between the change in evaluation phase arousal and the change in Payne index (Spearman rank correlation: N =19; $\rho_s =$ -0.528; P =0.020). Changes in evaluation phase arousal did not systematically vary with changes in the frequency of choosing the safe option (Spearman rank correlation: N =20; $\rho_s =$-0.004; P=0.987) or with the changes in Payne index (Spearman rank correlation: N =20; $\rho_s =$-0.208; P=0.380) for the group that experienced low changes in pretrial arousal from the high hypothetical to the high real block. Our results provide support for the synergy between tonic (pretrial) and phasic (evaluation phase) arousal (*57*).

Supplementary Figures

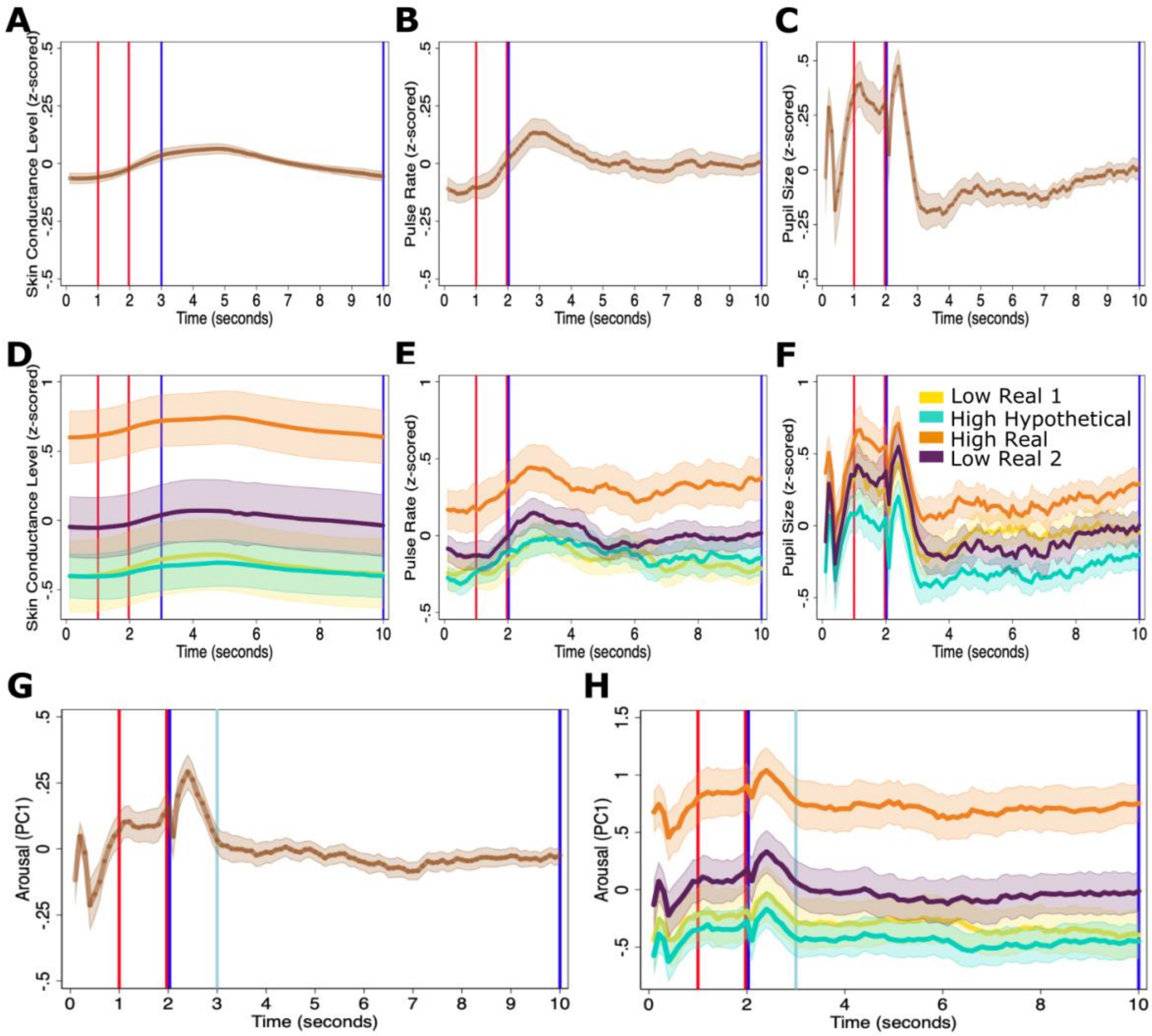

Fig. S1. Mean skin conductance, pulse rate and pupil size when viewing the fixation cross and during the evaluation phase. (A) Mean skin conductance level and **(B)** mean pulse rate across time in a trial for all participants and trials. **(A-B)** For each 100 milli-seconds, one datapoint is extracted by taking the average across 25 samples recorded. **(C)** Mean pupil size across time in a trial for all participants and trials. For each 100 milli-seconds, one datapoint is extracted by taking the mean across 100 samples recorded. Mean **(D)** skin conductance level, **(E)** pulse rate, and **(F)** pupil size across time in a trial for each block. All arousal measures are z-scored at the individual level across all trials. Mean **(G)** first principal component of the three arousal measures across time in a trial **(G)** for all participants and trials and **(H)** for each block. Pretrial measures are obtained as the one second average pre-stimulus presentation (red bounds) while evaluation phase measures are obtained post-stimulus presentation and prior to the selection phase (blue bounds). Evaluation phase skin conductance (skin conductance response- SCR) is derived as the maximum recorded response by trough-to-peak amplitude difference (squared-root transformation applied) in the time window 1 second after stimuli presentation till 8 seconds from onset (blue bounds starting at the light blue edge). Evaluation phase pulse rate is derived by subtracting the pretrial pulse measure from the 8 second average post-stimulus presentation (prior to selection phase). Evaluation phase pupil size is derived by subtracting the pretrial pupil measure from the maximum pupil size during the 8 seconds post-stimulus presentation (prior to selection phase). The shaded region shows 95% confidence intervals around the mean value for each measure.

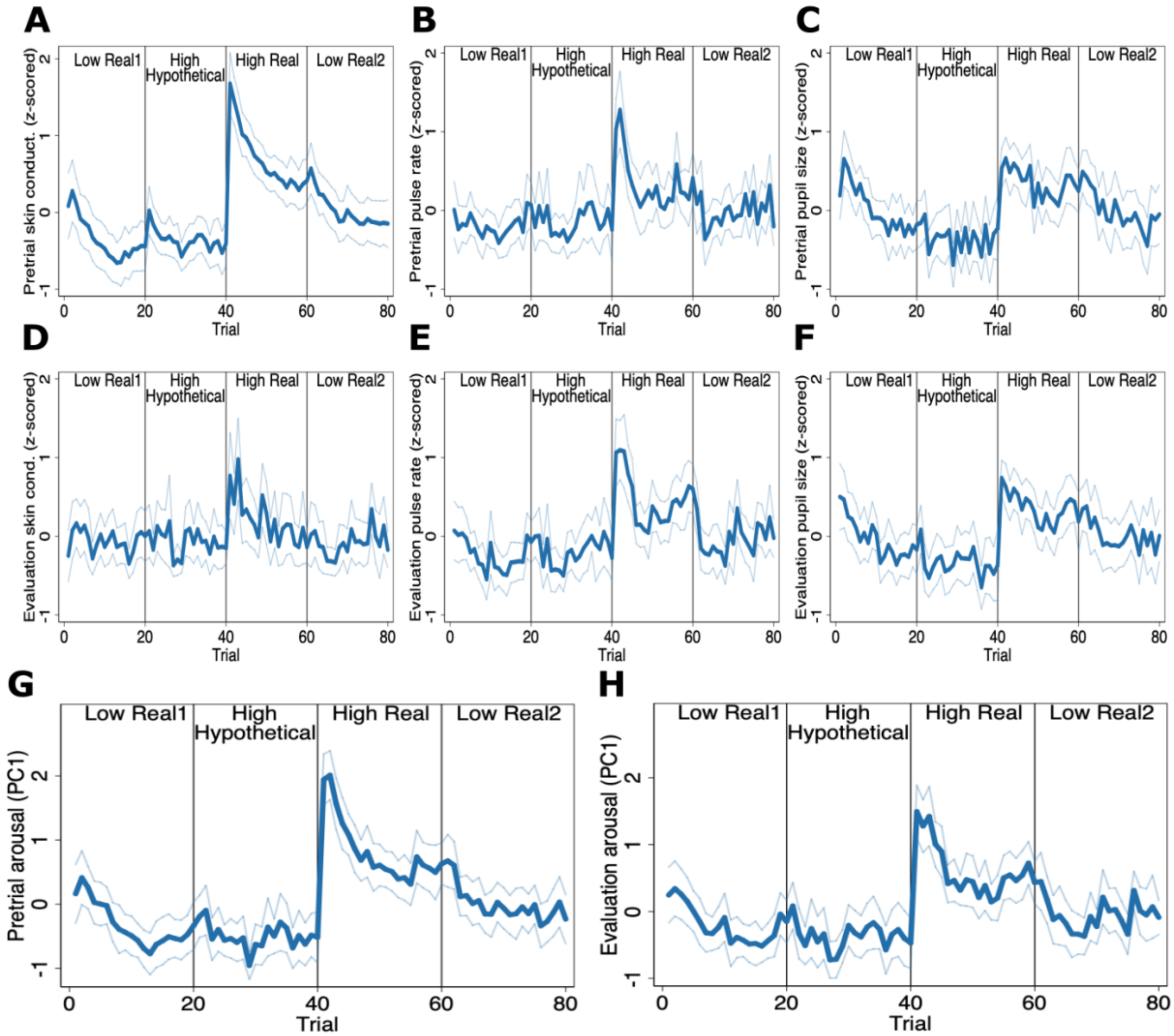

Fig. S2. Mean skin conductance, pulse rate and pupil size across trials. Mean pretrial **(A)** skin conductance level, **(B)** pulse rate, and **(C)** pupil size are plotted against trials during the experimental session. Mean evaluation phase **(D)** skin conductance response, **(E)** pulse rate, and **(F)** maximum pupil size are plotted against trials during the experimental session. Decisions within a block were randomized across participants. **(G)** Mean first principal component across pretrial skin conductance level, pulse rate, and pupil size and **(H)** mean first principal component across evaluation phase skin conductance response, pulse rate, and maximum pupil size are plotted decisions during the experimental session. All measures are z-scored at the individual level across all trials. Line bounds show 95% confidence intervals.

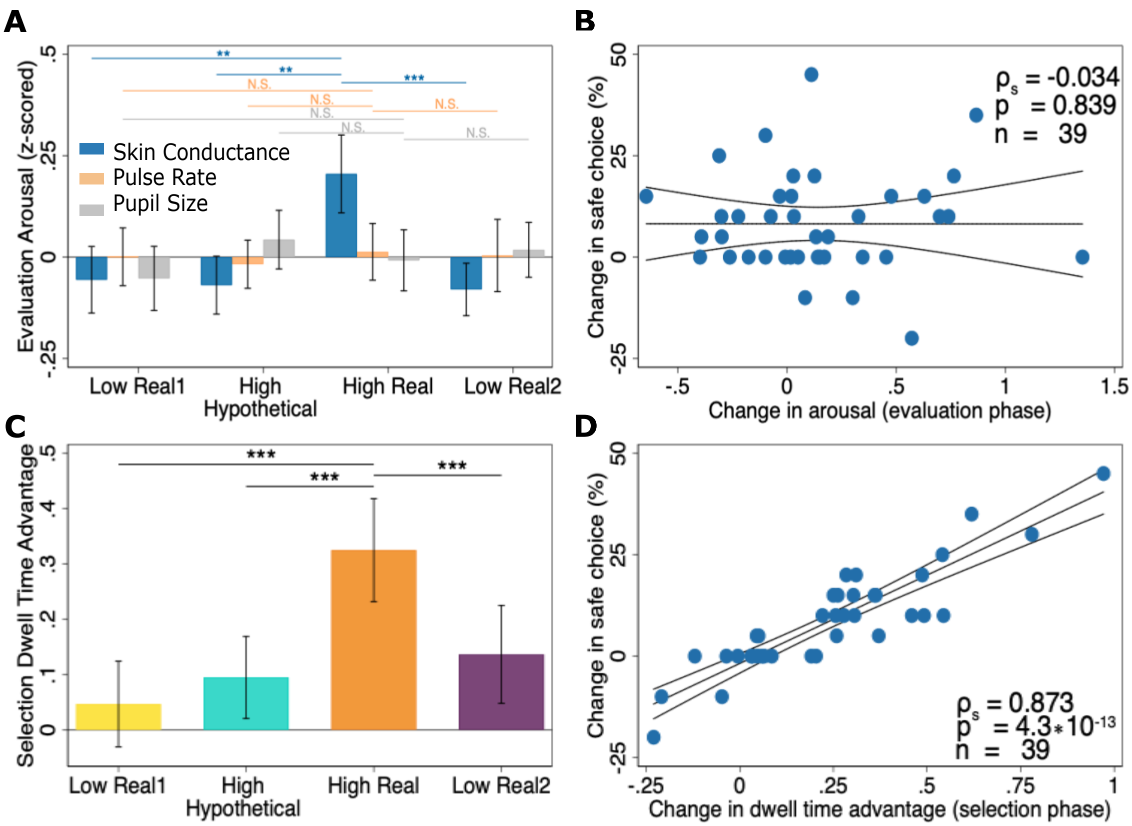

Fig. S3. Incentives, (evaluation phase) arousal and (selection phase) attention. (A) Only skin conductance response was higher under high real stakes while evaluation phase pulse rate and pupil diameter (phasic measures) did not significantly differ across blocks. **(B)** Individual differences in the effect of high stakes on generalized evaluation phase arousal were not associated with changes in implied risk aversion. The percentage difference in safe choices (y-axis) in the high real vs. the hypothetical block is plotted against the change in evaluation phase arousal (x-axis). Generalized evaluation phase arousal is computed as the first principal component of the three phasic arousal measures: skin conductance response, pulse rate and pupil size (Spearman rank correlation reported). **(C)** Dwell time advantage during the selection phase for the safe option (relative fixation duration on safe outcomes minus risky outcomes) was highest during the high real block. **(D)** Individual differences in the effect of high stakes on dwell time advantage for the safe option in the high real vs. the hypothetical block (x-axis) during the selection phase were strongly associated with changes in risk aversion (y-axis). Spearman rank correlation and linear fits plotted in **(B)** and **(D)**. Error bars and line bounds show 95% confidence intervals. For **(A)** and **(C)**, Wilcoxon signed-rank test (N=39): ** P-value < 0.01; *** P-value < 0.001; N.S. not significant.

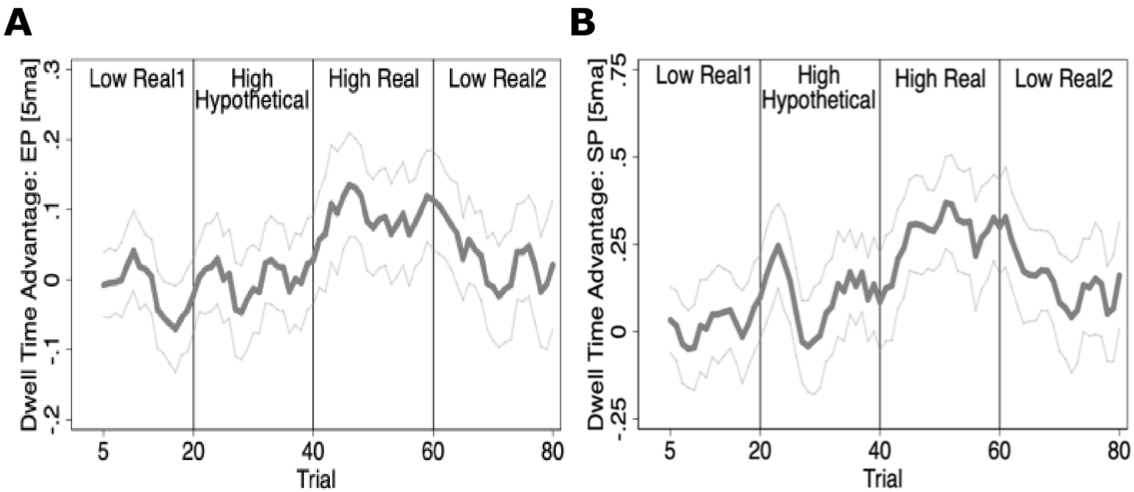

Fig. S4. Gaze bias across trials. Five trial moving average of dwell time advantage for the safe option during **(A)** evaluation phase and **(B)** selection phase are plotted against trials during the experimental session and spike at the beginning of the high real block.

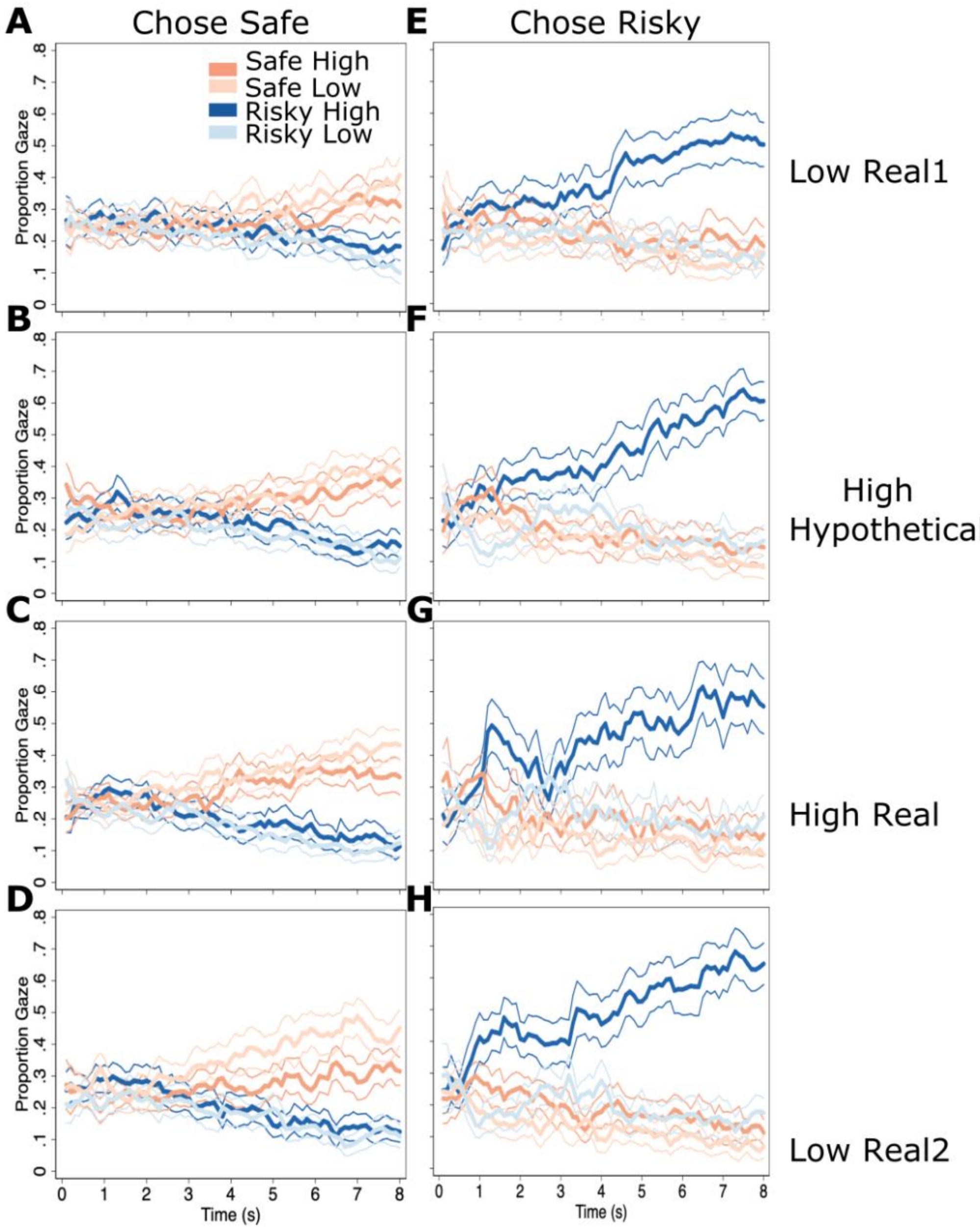

Fig. S5. Attention during the evaluation phase across blocks. Cumulative proportion, by blocks, of the evaluation phase with gaze fixated on each outcome and associated probability when participants (**A-D)** chose the safe option and (**E-H)** chose the risky option. Error bars and line bounds show 95% confidence intervals.

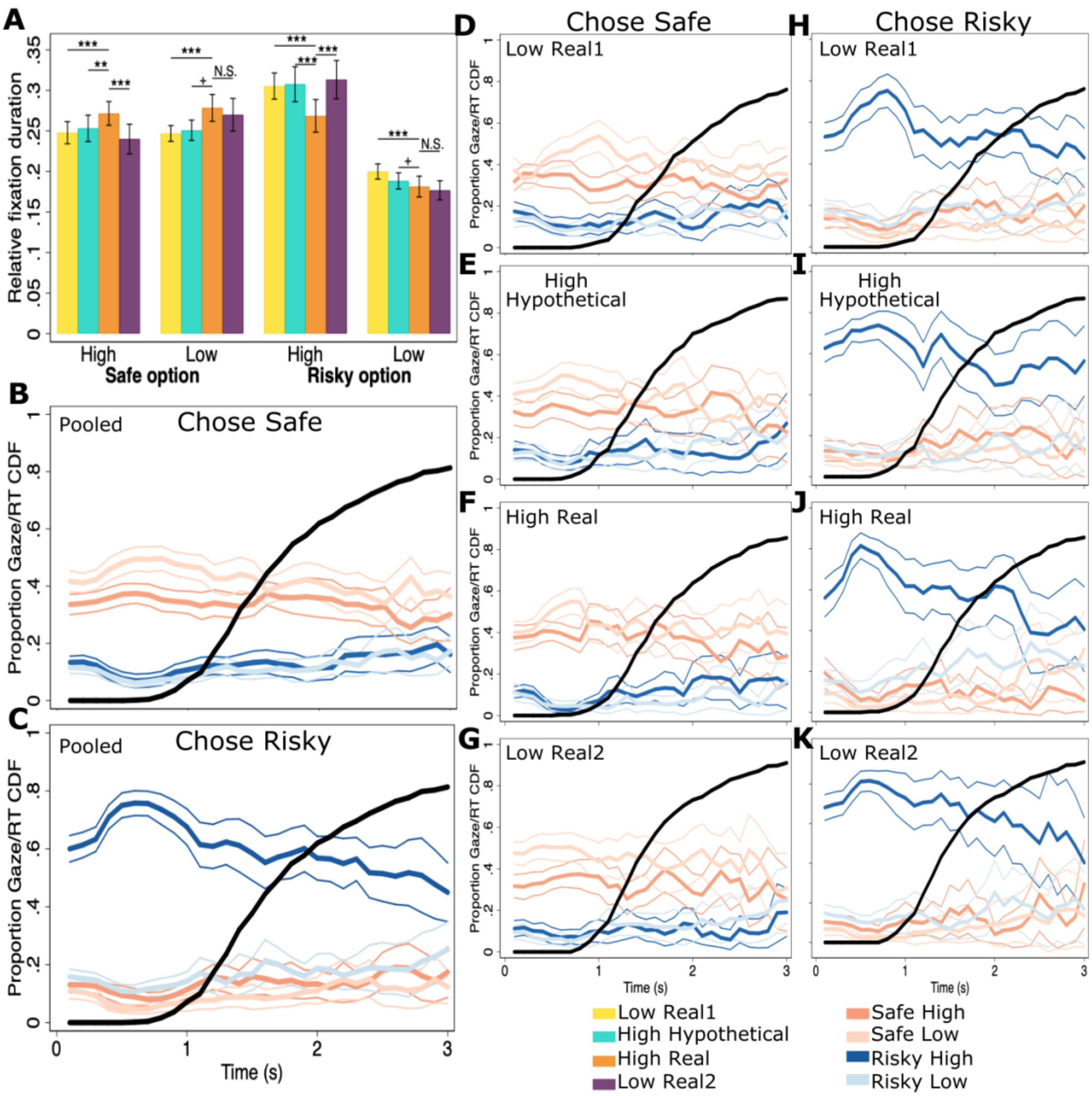

Fig. S6. Attention during selection phase. **(A)** Selection phase relative fixation duration (dwell-time proportion) on each outcome and associated probability during the evaluation phase. Fixation duration on the risky high outcome decreased in the high real block relative to the other three blocks. Cumulative proportion of the evaluation phase with gaze fixated on each outcome and associated probability when participants **(B)** chose the safe option and **(C)** chose the risky option across all blocks. Cumulative proportion, by blocks, of the evaluation phase with gaze fixated on each outcome and associated probability when participants **(D-G)** chose the safe option and **(H-K)** chose the risky option. Reaction time (RT) cumulative distribution function (CDF) is shown. Error bars and line bounds show 95% confidence intervals. Wilcoxon signed-rank test (N=39): + P-value <0.10; * P-value < 0.05; ** P-value < 0.01; *** P-value < 0.001; N.S. not significant.

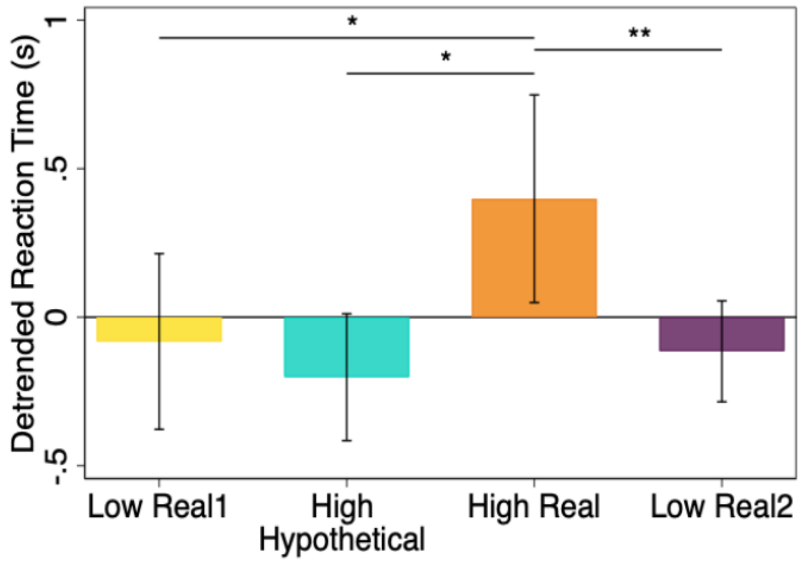

Fig. S7. Detrended reaction time. Average detrended reaction time across blocks. Quadratic time trend is applied. Error bars denote 95% confidence intervals. Wilcoxon signed-rank test (N=39): * P-value < 0.05; ** P-value < 0.01.

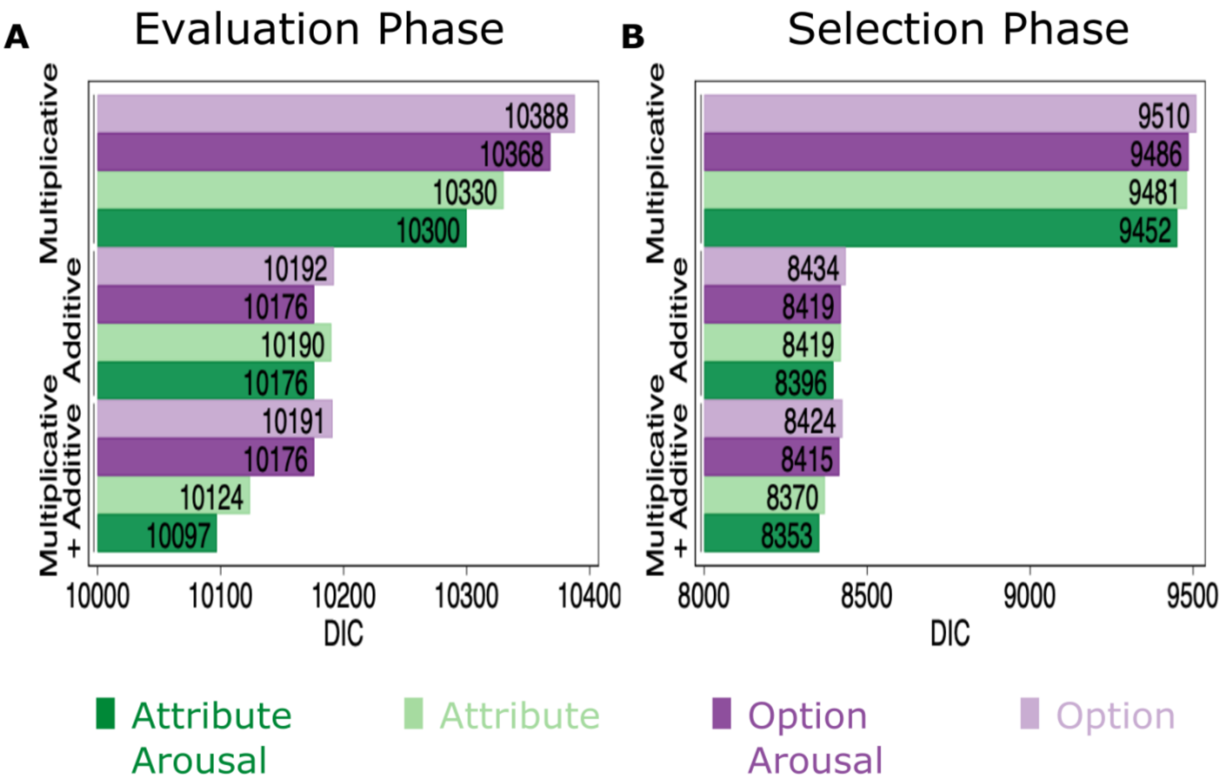

Fig. S8. Model fits for drift diffusion models. DIC for attribute-based and option-based models **(A)** with gaze recorded during evaluation phase and **(B)** with gaze recorded during the selection phase.

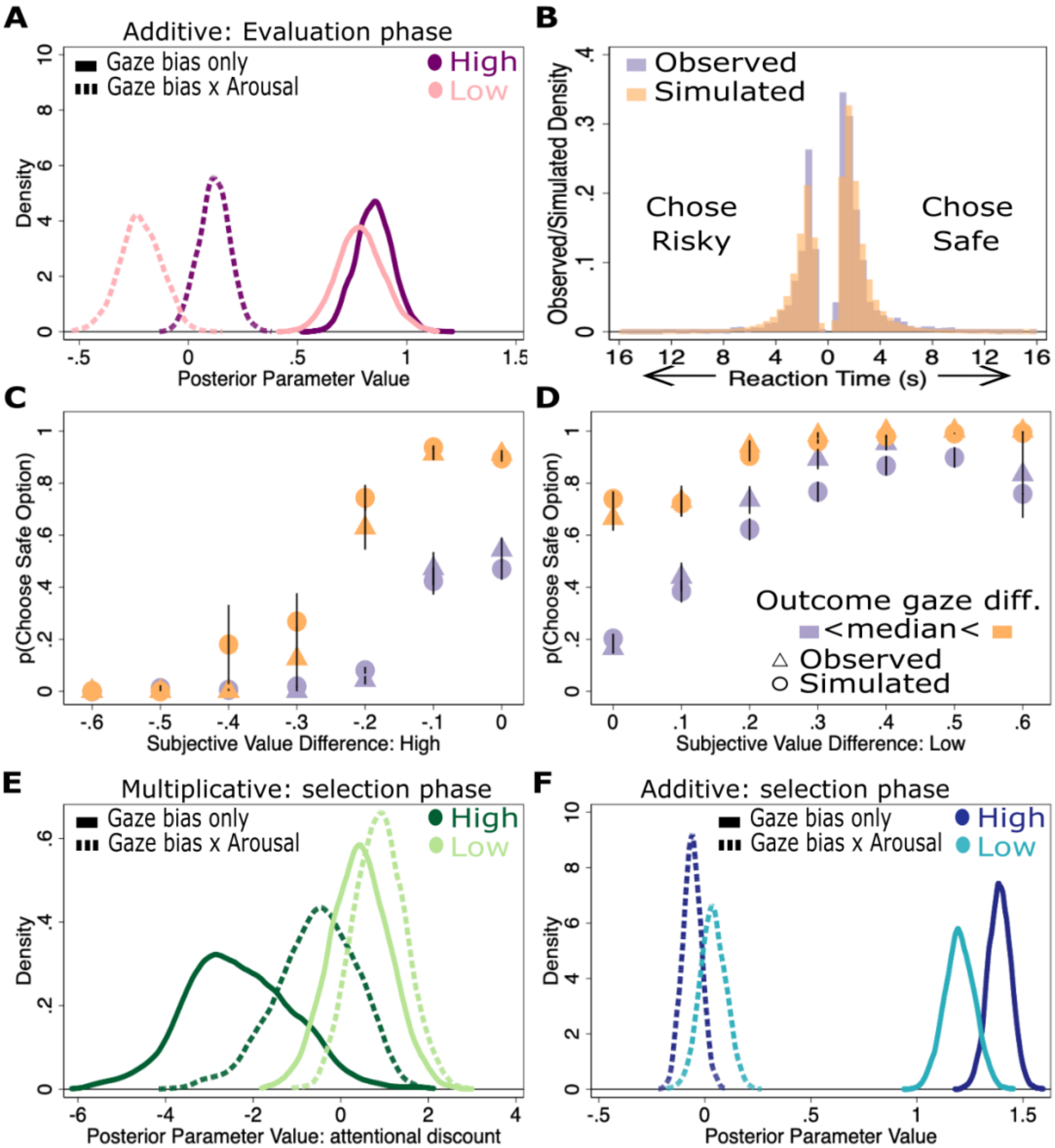

Fig. S9. Arousal-modulated Attentional Drift Diffusion Model: additive gaze bias and estimates from selection phase gaze. (A) Additive gaze bias for high and low attributes during evaluation phase ($\boldsymbol{\beta_{\Delta g_{high}} = 0.85, p < 0.0001}$; $\boldsymbol{\beta_{\Delta g_{low}} = 0.79, p < 0.0001}$), with arousal strengthening it for high attributes and weakens it for low attributes ($\boldsymbol{\beta_{pc1*\Delta g_{high}} = 0.12, p = 0.053}$; $\boldsymbol{\beta_{pc1*\Delta g_{low}} = -0.22, p = 0.01}$). Simulated choices from the best fitting model (model SE6PC1) with selection phase gaze predicted **(B)** reaction time and **(C)** observed choices relative to the high outcomes' value difference, and **(D)** the low outcomes' value difference. Error spikes denote the standard error of the mean. Extreme outlier reaction times are not shown in **(B)**, less than 1.3% of the data points are omitted. **(E)** Gaze on the opposite outcome during the evaluation phase discounted the value of the high outcomes only ($\boldsymbol{\gamma_{high}}$= -2.32, P (1-pd)=0.032). Arousal has no significant effect when interacted with multiplicative selection phase gaze. **(F)** Additive gaze bias for high and low outcomes during selection phase ($\boldsymbol{\beta_{\Delta g_{high}} = 1.39, p < 0.0001}$; $\boldsymbol{\beta_{\Delta g_{low}} = 1.20, P\ (1 - pd) < 0.0001}$). Arousal had no significant effect when interacted with additive selection phase gaze bias.

Supplementary Tables

Decision	Option A: Safe				Option B: Risky				EV diff.
Outcome	High		Low		High		Low		
#	%of A1	$A1	%of A2	$A2	%of B1	$B1	%of B2	$B2	
1	10%	2	90%	1.6	10%	3.85	90%	0.1	1.165
2	20%	2	80%	1.6	20%	3.85	80%	0.1	0.830
3	30%	2	70%	1.6	30%	3.85	70%	0.1	0.495
4	40%	2	60%	1.6	40%	3.85	60%	0.1	0.160
5	50%	2	50%	1.6	50%	3.85	50%	0.1	-0.175
6	60%	2	40%	1.6	60%	3.85	40%	0.1	-0.510
7	70%	2	30%	1.6	70%	3.85	30%	0.1	-0.845
8	80%	2	20%	1.6	80%	3.85	20%	0.1	-1.180
9	90%	2	10%	1.6	90%	3.85	10%	0.1	-1.515
10	100%	2	0%	1.6	100%	3.85	0%	0.1	-1.850

Table S1. Holt & Laury (2002) choices (lowest stakes: 1X), expected value difference was not provided to participants.

		High outcomes				Low outcomes				Additive		Arousal
Model	$\boldsymbol{\beta_0}$	$\boldsymbol{\beta_{H_{sameO_{sameA}}}}$	$\boldsymbol{\beta_{H_{sameO_{otherA}}}}$	$\boldsymbol{\beta_{H_{otherO_{sameA}}}}$	$\boldsymbol{\beta_{H_{otherO_{otherA}}}}$	$\boldsymbol{\beta_{L_{sameO_{sameA}}}}$	$\boldsymbol{\beta_{L_{sameO_{otherA}}}}$	$\boldsymbol{\beta_{L_{otherO_{sameA}}}}$	$\boldsymbol{\beta_{L_{otherO_{otherA}}}}$	$\boldsymbol{\beta_{\Delta g_{high}}}$	$\boldsymbol{\beta_{\Delta g_{low}}}$	$\boldsymbol{\beta_{pc1}}$
1A: Evaluation Phase	**0.09 (0.03)**	**4.68 (0.41)**	**1.47 (0.61)**	**4.06 (0.45)**	**2.32 (0.58)**	**3.22 (0.33)**	**2.18 (0.34)**	**2.38 (0.43)**	**4.41 (0.38)**	**0.85 (0.09)**	**0.79 (0.11)**	**0.04 (0.02)**
		Variables interacted with arousal (pc1)										
		0.39 (0.35)	**-1.20 (0.54)**	**0.75 (0.37)**	**-1.76 (0.51)**	**-0.51 (0.28)**	**-0.41 (0.34)**	**-0.27 (0.28)**	**-0.09 (0.29)**	**0.12 (0.07)**	**0.22 (0.10)**	
1B: Selection Phase	**0.10 (0.03)**	**2.38 (0.24)**	**0.90 (0.52)**	**2.24 (0.28)**	**1.40 (0.52)**	**1.69 (0.20)**	**1.28 (0.23)**	**1.73 (0.27)**	**2.57 (0.26)**	**1.28 (0.03)**	**1.05 (0.04)**	**-0.02 (0.02)**
		Variables interacted with arousal (pc1)										
		-0.39 (0.19)	**-0.57 (0.39)**	**-0.27 (0.21)**	**-0.65 (0.40)**	**-0.39 (0.18)**	**0.10 (0.19)**	**-0.46 (0.20)**	**-0.06 (0.22)**	**-0.08 (0.03)**	**0.07 (0.03)**	

Table S2. Drift rate regression estimates for models SE6 with (1A) evaluation phase gaze and (1B) with selection phase gaze: Mean (SD)